Vehicle Wheel Energy Reduction at Intersections using Signal Timing and Adaptive Cruise Control

Dillon P. Scott

Thesis submitted to the Faculty of the
Virginia Polytechnic Institute and State University
in partial fulfillment of the requirements for the degree of

Master of Science
in
Mechanical Engineering

Douglas J. Nelson
Steve C. Southward
Thomas E. Diller

May 5, 2022
Blacksburg, Virginia

Keywords: Cruise Control, Adaptive Cruise Control, Energy, Vehicle, Model Predictive Control, Signal Phase and Timing

Vehicle Wheel Energy Reduction at Intersections using Signal Timing and Adaptive Cruise Control

Scott P. Dillon

(ABSTRACT)

The Hybrid Electric Vehicle Team (HEVT) at Virginia Tech participates in the 4-Year EcoCAR Mobility Challenge organized by Argonne National Laboratory. The objective of this competition is to modify a stock 2019 internal combustion engine Chevrolet Blazer and incorporate a hybrid powertrain and advanced driver assist systems. The Blazer has a P4 hybrid architecture which contains an electric traction motor on the rear axle and an internal combustion engine on the front axle. HEVT seeks to develop a vehicle with advanced driving capabilities to demonstrate energy savings by utilizing existing technologies. The hybrid market has generally been tailored to small compact vehicles however, a Chevrolet Blazer is a midsize utility vehicle that offers additional space with the benefit of increased fuel economy.

The research discussed in this paper focuses on the design of a Signalized Intersection Control Strategy. First, research is performed on different methods of intersection control and implementation with an existing Model Predictive Adaptive Cruise Controller. Based on ease of integration into an existing tuned Eco Adaptive Cruise Control System (ACC), a control strategy operating in the background of the main vehicle controllers is chosen. The main topic of this research is the development and simulation of a Signalized Intersection Control Strategy that works through an Eco ACC system to achieve further energy savings during an approach to a connected intersection while ensuring rider safety. This paper expands on the current knowledge of vehicle utilization of Signal Phase and Timing (SPaT) signals through simulated test cases of a vehicle system model using MATLAB. In each case, the tractive energy consumption and travel times are analyzed for both the Eco ACC system with Signalized Intersection Control Strategy (informed) vehicle and an assumed uninformed driver for comparison. In the case of a vehicle approaching a green intersection which turns red several seconds after SPaT information is received, the informed system shows a 92% decrease or 75 Wh/mi reduction in propel energy consumption at when compared to an uninformed driver. However, in a similar case where the vehicle accelerates back to cruising speed after the light turns green, displays only an 11% decrease or 47 Wh/mi reduction in propel energy consumption at the wheel when compared to the uninformed driver. These simulations confirm that the Signalized Intersection Control Strategy reduces the propel energy consumption at the wheel during approaches to signalized intersections without extending the travel time greatly and in some cases at all. The results of this research show that the control strategy reduces tractive energy consumption while maintaining travel time.

Vehicle Wheel Energy Reduction at Intersections using Signal Timing and Adaptive Cruise Control

Scott P. Dillon

(General Audience Abstract)

The Hybrid Electric Vehicle Team (HEVT) at Virginia Tech participates in the 4-Year EcoCAR Mobility Challenge organized by Argonne National Laboratory. The objective of this competition is to change a stock 2019 internal combustion engine Chevrolet Blazer into a functioning hybrid. This conversion is accomplished with the addition of an electric motor to allow the vehicle to burn less gasoline and increase customer appeal. The hybrid market has generally been tailored to small compact vehicles however, a Chevrolet Blazer is a midsize utility vehicle that offers additional space with the benefit of increased fuel economy.

The research discussed in this paper focuses on the design of a Signalized Intersection Control Strategy. First, research is performed on various methods of existing intersection speed control. Based on ease of integration, a background process is chosen to update the set speed of the vehicle. The main topic of this research is the development and simulation of a Signalized Intersection Control Strategy that achieves greater energy savings during approaches to intersections. This paper expands on the current knowledge of vehicle utilization of Signal Phase and Timing (SPaT) signals through simulated test cases of a vehicle system model using MATLAB. In the case of a vehicle approaching a green intersection which turns red several seconds later, the implemented strategy shows a 92% decrease in energy consumption when compared to an uninformed driver. However, a similar case where the vehicle accelerates back to cruising speed after the light turns green displays only an 11% decrease in energy consumption when compared to an uninformed driver. These simulations confirm that the Signalized Intersection Control Strategy successfully reduces energy consumption without significant travel time extensions. The results of this research show that the control strategy reduces tractive energy consumption while maintaining travel time.

Contents

List of Figures

List of Tables

Chapter 1

Introduction

The EcoCAR Mobility Challenge is a four-year design competition that challenges students to convert a stock 2019 Chevrolet Blazer RS to a hybrid vehicle with team-selected sensors and processors for Connected and Automated Vehicles (CAVs) features. As part of the competition, the Hybrid Electric Vehicle Team (HEVT) implemented a P4 hybrid architecture. In a hybrid P4 configuration, the torque-producing component on the rear axle is separate from the torque-producing component on the front axle. Additionally, the stock V6 engine in the Blazer was replaced with a General Motors 2.5L naturally aspirated inline four-cylinder engine, which can provide 144kW of peak power to the front axle. The rear axle is powered by an 50kW electric traction motor electrically coupled to a 5.4KWh battery pack.

In addition to integrating a hybrid propulsion system, HEVT modified the vehicle with sensors and computational hardware to enable vehicle autonomy and connectivity. The integrated hardware was used to develop an Adaptive Cruise Control (ACC) system, which automatically changes the Ego vehicle speed to match the velocity of a lead vehicle in its trajectory. The first three years of the EcoCAR Mobility Challenge focused on sensor selection, algorithm development, and testing for the ACC system. For the fourth and final year of the competition, teams were challenged to integrate Vehicle-to-Infrastructure (V2I) connectivity into their existing ACC systems. The primary objective of integrating V2I is to reduce the amount of time spent stopped at a red light, thereby reducing energy consumption [12].

This work is driven by a major EcoCAR Mobility Challenge goal of reducing energy consumption. In recent years, the federal government raised fuel economy requirements in an effort to reduce the amount of emitted greenhouse gases. The impact has been reflected by continued decreases in emissions[2]. By integrating V2I capabilities using a Signalized Intersection Control Strategy, HEVT seeks to further reduce energy consumption.

When discussing add-on control schemes, some base knowledge of the current vehicle architecture and control capabilities is necessary. There are several controllers in a stock vehicle that will interact with a standard cruise controller and its requests for axle torque. However,

HEVT has added several aftermarket controllers used in the processing and implementation of vehicle Adaptive Cruise Control (ACC).

"The CAVs sensor fusion is responsible for processing information from the camera and radar which includes object and lane tracking. The Bosch mid-range radar has a range of 160 meters, varying field of view of 20° below 60 m, and is limited to 12° at the maximum range. The camera sensor is a Mobileye Intelligent vision system with a range of 80 m and field of view of 100°" [1]. The sensor fusion anglorth is responsible for combining all sensor data and reporting the most important object to the CAVs processing unit (Intel Tank) for use in autonomous driving. The CAVs processing unit reports the range of the most important object along with range rate.

The CAVs processing unit is responsible for running HEVT's Adaptive Cruise Control algorithm and Signalized Intersection Control Strategy. The Hybrid Vehicle Supervisory Controller (Propulsion System Controller) takes brake or acceleration requests from either the automated vehicle systems or driver and implements the desired performance through lower level controllers. The Hybrid Vehicle Supervisory Controller (HVSC) utilizes a torque split strategy to increase fuel economy by selecting when and how much power to request from either powertrain system at any given time. By utilizing two separate powertrains in combination, increased performance and fuel economy can be achieved.

Figure 1.1 outlines the interface between the CAVs supervisory controller, Propulsion System Controller, and vehicle systems.

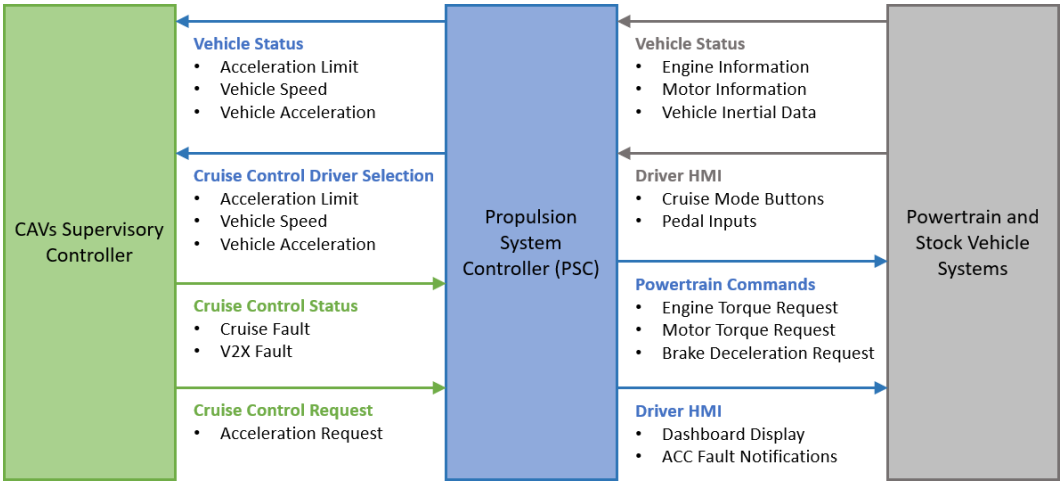

Figure 1.1: Overview of the Vehicle Control Architecture.

This research is centered on creating a Signalized Intersection Control Strategy that functions with the help of an Eco ACC system with validation through MATLAB simulations. These simulations primarily focus on a single vehicle (Ego Vehicle) as it approaches a signalized intersection. The Signalized Intersection Control Strategy is implemented to update the set speed of the vehicle over every time step during simulation. The Eco ACC system

developed by Tim Ryan [1] utilizes this set speed and allows the vehicle to follow a chosen trajectory accordingly. Under the assumption of properly processes sensor fusion data, the Eco ACC system prevents collisions through verified simulation cases in MATLAB. These scenarios include city driving and faster test conditions with connected intersections. Once the Signalized Intersection Control Strategy is verified, its integration into the Eco ACC system is tested to ensure no significant change in rider comfort. The scope is to verify additional energy savings through the combination of an existing Eco ACC system and one with SPaT information. Specifically, the Signalized Intersection Control Strategy should not impede on the safety and rider comfort of the existing Eco ACC system. Comfort is a analyzed by observing the Ego vehicle acceleration and jerk.

The MATLAB simulations also estimate vehicle tractive energy at the wheel to analyze whether improvements in energy consumption can be achieved without compromising the safety of the ACC system. Rather then looking into powertrain efficiencies, emphasis is placed on investigating tractive energy usage at the wheels so these findings are relevant for vehicles with different powertrain applications. Reducing tractive energy consumption at the wheel lowers fuel consumption in a traditional Internal Combustion Engine and reduces battery energy consumption for a Battery Electric Vehicle [17]. Since the methods used for reducing energy consumption only utilize acceleration requests, the same techniques can be applied to different vehicles as they do not rely on specific vehicle parameters. The scope does not involve the implementation and testing of the Signalized Intersection Control Strategy on any vehicle. The overall objectives of this work are to integrate a Signal Phase and Timing controller into an Eco ACC system to improve energy consumption at and nearing connected intersections, maintain the rideability standards of the Eco ACC system, and to maintain or improve travel time through various simulated scenarios.

This research includes the following sections. Chapter 1 reviews the topic of Model Predictive Control with Signalized Intersection information by reviewing recent literature. Then, the vehicle dynamics are discussed to provide background information for energy comparisons and controller implementation. Chapter 2 discusses the Eco MPC ACC system developed by Ryan [1] and how this system works in conjunction with the Signalized Intersection Control Strategy being developed. Chapter 3 discusses the simulation and energy consumption of a vehicle with and without prior knowledge of traffic light information. Chapter 4 describes the conclusions and suggested future work.

The topics presented in this research lead to the creation and simulation of the Signalized Intersection Control Strategy.

1.1 Literature Review

1.1.1 Holistic MPC Control Scheme

The paper written by Niklas Wikström [21], delves into the development of an all encompassing MPC controller designed to incorporate not only a lead vehicle but also traffic lights, road speed limits, gradients, and curvature. He starts by giving an introduction into what ACC is as well as additional concepts related to the subject matter. He then defines the discrete time state space model used throughout which incorporates vehicle longitudinal position, velocity, and acceleration.

Wikström steps through the creation of the MPC controller matching each case (lead vehicle, traffic lights,...) with its associating set of constraints and weight policy. By addressing each sub-problem separately, Wikström allows readers to adapt separate sections of his work for their own purposes without the need to dissect the entire controller. While Wikström does show some promising results, he only covers one specific city driving scenario. He was able to model an energy saving of 10.3% - 29.8% depending on the Signal Phase and Timing scenarios he created for simulation. These increases in energy savings are when the holistic controller is compared to an assumed uninformed human driver with both taking the same amount of time to traverse the simulated distance.

While Wikström does present a good argument for the development of the MPC controller discussed, he does not discuss some import aspects of fuel savings specifically at signalized intersections. In the simulation he discusses there are only minor actions taken when braking vs. accelerating so the vehicle does not violate a red light condition. While this methodology is shown to simulate an improved energy consumption over a human driver there is still some energy savings potential that can be achieved. One such method that will be discussed during this paper is vehicle coasting (zero tractive energy at the wheel). If the conditions are met this method will allow for even greater potential energy savings.

1.1.2 ACC MPC with SPaT MPC

Sai Chada [6] reviews the current driving factors behind the on going desire to add advanced driver assistance systems specifically into electric vehicles. He states that electric vehicles are considered environmentally friendly, but there is current and on going research into systems that can further reduce electric vehicle energy consumption. While the vehicle discussed in this paper is a hybrid electric vehicle the driving factors remain the same (reduced energy consumption).

Chada explores three different scenarios in which to utilize his car following MPC and SPaT MPC controllers. These include: if there is no lead vehicle the car must pass through

the stop light during a green light, if there is a lead vehicle in range the Ego vehicle must track the lead vehicle in an energy-optimal manner, and if the upcoming stoplight is red the Ego vehicle must stop in an energy efficient manner at the stop line. Implementing a switching controller, using a state flow diagram, Chada can select the cases in which to use car following MPC or SPaT MPC. Rather then using two separate MPC controllers, the research discussed in this paper utilizes an existing Eco ACC MPC controller with live updates in set speed to follow an energy efficient path utilizing SPaT information.

He then presents an approximation of the electric vehicle power consumption map. By relating tractive force to velocity, power consumption can be derived. This is particularly useful when modeling electric vehicles with MPC controllers that work through optimization techniques. While the vehicle discussed in this paper is a hybrid electric vehicle, a similar approach could be taken in order to optimize power consumption.

Chada then displays the results of his simulation tests. Firstly, he demonstrates that an MPC controller with SPaT information can accumulate an energy savings anywhere from 19% to 26%. This simulation specifically compared the MPC controlled vehicle to vehicles under set speed controllers traversing six intersections with an approximate total length of 3.5 km. Chada's ACC MPC is also tested in a similar manner displaying an energy saving potential up to 13%. Next, Chada shows the results of the combined controllers in a simulation. The switching algorithm works properly which successfully reduces the energy consumption of the Ego vehicle. Chada claims that the system he developed is suited for real-time operation. However, being able to utilize a single Eco ACC MPC controller with Signalized Intersection Control Strategy may show better energy consumption reduction.

1.1.3 GLOSA

Joseph Tario [23] discusses several technologies and their uses in adaptive Eco-driving for traffic signal control. One of the more prominent techniques discussed in his paper and in current literature is the Green Light Optimal Speed Advisory (GLOSA) System. The goal of the GLOSA system is to provide a driver with speed recommendations near intersections in an effort to optimize fuel economy. This current system is just a recommendation and would require the driver to comply unless integrated through an adaptive cruise control system. A vehicle can receive speed advisory updates from a single GLOSA system and traffic light at any given time. The GLOSA algorithm works by utilizing a vehicles current position and speed, along with the position and signal timing of the nearest downstream intersection.

The main task of the algorithm is to find the best decision among several common scenarios. These include, do nothing to pass the intersection, acceleration to pass, decelerate to pass, and decelerate to stop. When a vehicle enters the range of the intersection, the system checks the validity of the four scenarios discussed and suggests the best possible path for the driver to follow. In the case of a full stop being required, Tario claims that there is no scope to optimize fuel economy in this case so the algorithm picks a steady deceleration rate to get

the vehicle to the stop line.

The research discussed in this paper operates in a similar manner to the GLOSA system while improving its eco approaches through coasting. Utilizing the known vehicle speed and the broadcast SPaT information by Vehicle to Infrastructure communication protocols, an eco approach to the stop light can be made. While the GLOSA system is well thought out and robust, there is room for improvement specifically when the vehicle has to come to a complete stop. This is one of the major points being looked at in this research.

1.1.4 Engine Cutoff Coasting

Brown's research on active engine-off coasting [5] describes the fuel savings achievable during coasting. Engine-off coasting is the method of turning the engine off while also forcing the transmission into neutral (passive engine-off coasting). This physically disconnects the transmission from the driveshaft and reduces energy loss with the car not idling. Brown discusses both passive engine-off coasting and active engine-off coasting. Active engine-off coasting is performed with the use of a small electric motor supplying power to the wheels to overcome aerodynamic drag.

Brown tests the methods discussed by changing the stored energy size which directly impacts the cruising length obtainable. The overall benefits and testing of passive coasting near signalized intersections is further analyzed in this research. The passive and active engine-off methods display energy savings and CO_2 reduction. The outcome of this research applies to the HEVT vehicle discussed because the vehicle has separate electric and conventional powertrain systems that act independently.

1.2 Vehicle Dynamics

A common model for describing vehicle dynamics is the bicycle model. A 2-dimensional bicycle model accounts for lateral and longitudinal motions. The 2D bicycle model includes rotation of the vehicle around a center of mass and forces acting on both a front and rear tire [7]. However, for the work discussed in this paper, only the longitudinal direction is necessary. Dynamic equations are generated utilizing the vehicle free body diagram. Figure 1.2 displays the nominal forces acting on the free body diagram. Figure 1.2 also shows the tractive forces as the tires for the rear and front, F_{Tr} and F_{Tf}. This figure also shows the rolling resistance on the front and back F_{rf}, and F_{rr}, aerodynamic drag F_{aero}, grade F_{grade}, as well as the inertial force acting on the center of mass.

A force balance equation along the x-axis using the free body diagram as seen in Eq. 1.1.

$$F_{Tr} + F_{Tf} = F_{rr} + F_{rf} + F_{aero} + F_{grade} + F_{inertia} \tag{1.1}$$

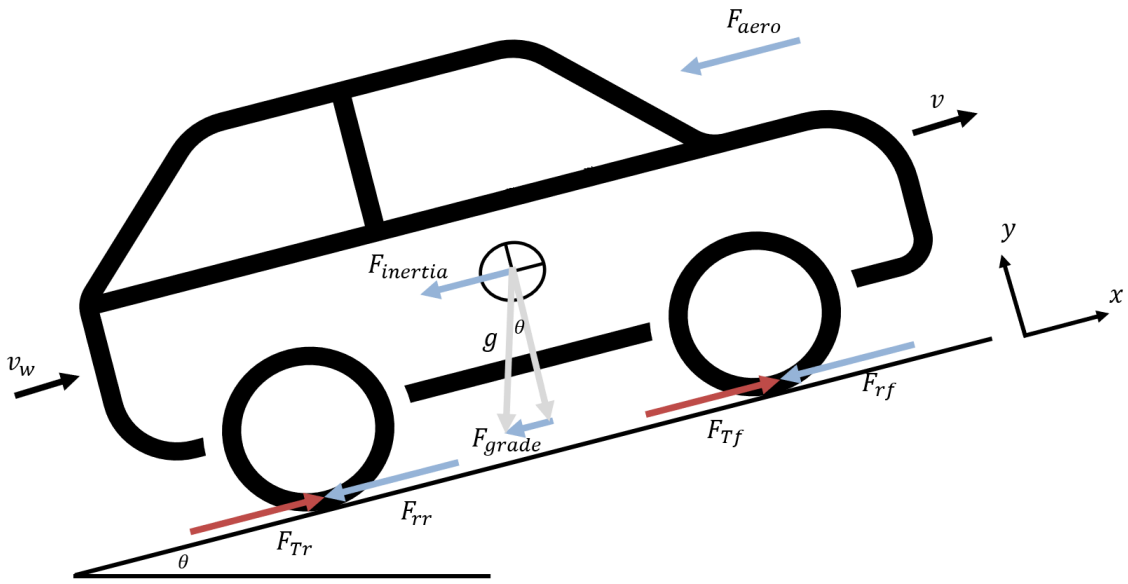

Figure 1.2: Simple Free Body Diagram Displaying the Nominal Forces Acting on a Vehicle.

A simplification of Eq. 1.1 leads to the presumption that combines rolling force and tractive force. The simplified equation can be seen below in Eq. 1.2.

$$F_T = F_r + F_{aero} + F_{grade} + F_{inertia} \tag{1.2}$$

The combined front and rear tractive forces and rolling resistances are represented by $F_T = F_{Tr} + F_{Tf}$ and $F_r = F_{rr} + F_{rf}$ respectively. F_{aero} is the aerodynamic drag, F_{grade} is the force due to gravity, and $F_{inertia}$ is force of inertia caused by acceleration. In the following sections the basics of each displayed force will be discussed along with the effects it has on the motion of the vehicle.

1.2.1 Rolling Resistance

The complex structure of the tire includes a synthetic polymer, many flexible filament cords, glass fiber, and a bond to a low modulus polymeric material [19]. It is necessary to understand the physics behind a tire so that an accurate model is developed as part of a vehicle control algorithm.

The rolling resistance of a tire is affected by the tire structure, material, temperature, road surface, inflation pressure, and the presence of liquids [11]. An empirical model is often used in engineering which can be computationally expensive [19]. In controls, a simple model with similarly high levels of accuracy is favored. The model used in this research are the

derived road load coefficients stated in the EPA test car list data. Rolling resistance, F_r, is represented by the following equation.

$$F_r = (C_{r,0} + C_{r,1}v)mg \tag{1.3}$$

v is the vehicle velocity, $C_{r,0}$ and $C_{r,1}$ are the coefficients of rolling resistance, g is the gravitational constant, and m is the mass of the vehicle. Although road and tire conditions may change affecting the coefficients, the controller utilized is able to accurately follow a desired set speed.

1.2.2 Aerodynamic Drag

Air resistance is one of many motion opposing forces experienced by a vehicle. This force, aerodynamic drag, contains components from both shape drag and skin friction [8]. Shape drag is caused by pressure differential in front of and behind a vehicle. The motion of a vehicle creates a low pressure zone behind the vehicle and consequently a high pressure zone in front opposing motion.

Air resistance is described below using a simple model.

$$F_{aero} = \frac{1}{2}\rho A_f C_D v^2 \tag{1.4}$$

A_f is the frontal area, ρ is air density, v is the vehicle velocity, and C_D is the drag coefficient. An important factor to consider when designing a car is the road load force which is defined below.

$$F_{rl} = F_r + F_{aero} \tag{1.5}$$

F_{areo} is the aerodynamic drag and F_r is the rolling resistance. Generally, when a vehicle is traveling slower then $20m/s$, the rolling resistance is the dominant force. However, at greater speeds the dominant force resisting motion is the aerodynamic drag.

1.2.3 Grade

Grade forces act on the vehicle when traveling in non-flat situations. This includes hills, mountains, or even very minor changes in elevation. Grade can be difficult to measure meaning a robust controller must be able to handle unknown disturbances. The grade at any time is either assisting with the motion of the vehicle (down hill), or resisting the motion of the vehicle (up hill) which will require more power from the vehicle to overcome. The force component of road grade is represented below.

$$F_{grade} = mg\sin\theta \tag{1.6}$$

m is the vehicle mass, θ is the road angle, and g is the gravitational constant. $\sin\theta$ is often referred to as the road grade. It is assumed, using small angle approximations, that $\sin\theta = \theta$ where θ is in radians.

It is common to claim that $\sin\theta$ is the grade of the road. Using small angle approximations of the road, it is assumed that $\sin\theta = \theta$ where θ is in radians.

1.2.4 Inertial Force

Inertial force is produced by the acceleration of the vehicle and mass of the vehicle. The inertial force is comprised of the rotating wheels and rotating powertrain components. The utilization of individual models for these components is generally unnecessary in vehicle control. $F_{inertia}$ is defined below.

$$F_{inertia} = \delta_I ma \tag{1.7}$$

δ_I represents the rotating inertia in the form of a correction factor, m is the vehicle mass, and the acceleration of the vehicle is represented by a. The inertial factor is written below.

$$\delta_I = 1 + \delta_1 + \delta_2 i_0^2 \tag{1.8}$$

δ_1 represents the intertia factor of the rotating wheel and is assumed to be 0.04. δ_2 is the intertia factor of the rotating powertrain components and is assumed to be 0.0025. The total combined inertial factor is estimated to be 1.04 [8]. $F_{inertia}$ is represented below with the combined inertial factor.

$$F_{inertia} = \delta_I ma = 1.04ma \tag{1.9}$$

a is the vehicle acceleration and m is the vehicle mass. Acceleration represents most the tractive forces present on a moving vehicle as shown by Figure 1.3. Aerodynamic drag plays a much larger role at higher speeds which is still no where close to the tractive forces acting on the vehicle due to inertial forces.

1.2.5 Vehicle Model

A complete vehicle model contains each aspect of the vehicle and the interactions with its surroundings. The single degree of freedom model only accounts for longitudinal motion. A more detailed equation based on Eq. 1.2 is seen below.

$$\frac{T_a}{R} = (C_{r,0} + C_{r,1}v)mg + \frac{1}{2}\rho A_f C_D v^2 + mg\sin\theta + \delta_I ma \tag{1.10}$$

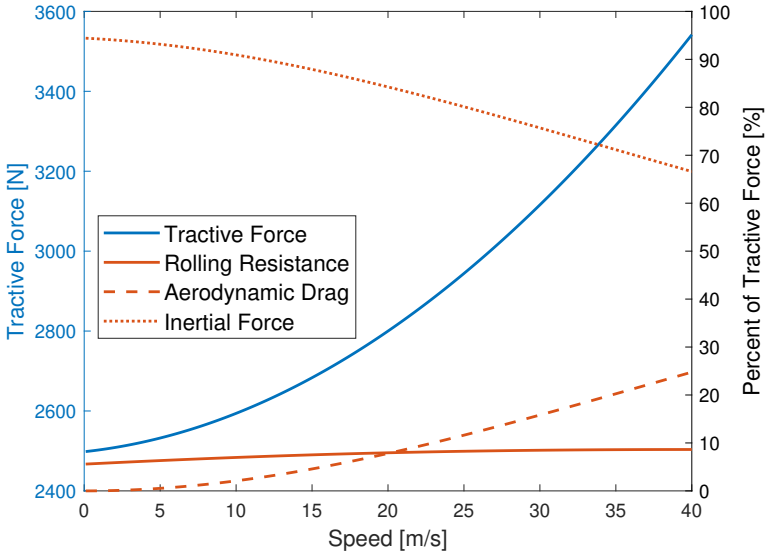

Figure 1.3: Road Load Forces Induced by 1 m/s^2 Acceleration Absent of Road Grade

The vehicle velocity is assumed to only travel in the positive direction, forward motion. Negative motion of the vehicle (backing up) is not considered in this model [18]. Derived from Eq. 1.10, a first order equation is created to show the that $a(t) = \dot{v}(t)$.

Relative position is important in the creation of an Adaptive Cruise Control algorithm. However, for a traditional cruise control algorithm tracking position is unnecessary. Utilizing Eq. 1.10, the 1st order differential equation can be seen below.

$$\dot{x} = -\frac{(C_{r,0} + C_{r,1}x)mg + \frac{1}{2}\rho A_f C_D x^2 + mg\sin\theta}{\delta_I m} + \frac{1}{\delta_I m R}T_a \tag{1.11}$$

$\dot{x} = \dot{v}(t) = a(t)$, $x = v(t)$, and T_a is the combined front and rear axle torque.

1.2.6 Vehicle Coefficients

Proper vehicle coefficient estimation is essential for a functional vehicle controller. The necessary components, road load coefficients, needed to find aerodynamic drag and rolling resistance are published each year by the Environmental Protection Agency. Vehicle fuel economy in both city and highway driving scenarios is published by the EPA. Road load coefficients and vehicle test masses are included in the published data [3].

The vehicle discussed in this research is a 2019 2.5L FWD Chevrolet Blazer. The vehicle parameters are found using a test mass of 4,250 lbs. The rest of the vehicle coefficients from the published EPA data are shown in both metric and imperial units below [3].

$$\begin{array}{llcll} \text{A} = & 26.65 & \text{lbf} & & f_0 = 118.5 \quad \text{N} \\ \text{B} = & 0.3552 & \text{lbf/mph} & \Longrightarrow & f_1 = 3.535 \quad \text{Ns/m} \\ \text{C} = & 0.02470 & \text{lbf/mph}^2 & & f_2 = 0.5503 \quad \text{Ns}^2\text{/m} \end{array}$$

The vehicle glider model used is shown below.

$$F_{rl} = f_0 + f_1 v + f_2 v^2 \tag{1.12}$$

Aerodynamic drag and rolling resistance are found from the glider equation shown below.

$$F_{rr} = f_0 + f_1 v = C_{r,0} mg + C_{r,1} mgv$$
$$F_{aero} = f_2 v^2 = \frac{1}{2} \rho A_f C_D v^2$$

Using the equations above, estimations for the Chevrolet Blazer parameters are shown in Table 1.1. These parameters are valid when the vehicle is traveling on a flat dry surface. For the purposes of this research it is assumed that the driving conditions are perfect and the terrain is flat. The Blazer being used by HEVT is heavier then the EPA test car list data. This is due to the integration of a high voltage energy storage system, electric rear traction motor, and various other computing hardware. These components, along with the addition of two passengers, bring the operation load of the vehicle to 2268 kg or 5,000 lbs.

Table 1.1: Blazer vehicle parameters

Parameter		
m	kg	2268
δ_I		1.04
$C_{r,0}$		0.00627
$C_{r,1}$	s/m	0.000187
C_d		0.330
A_f	m^2	2.78
R	m	0.378

1.2.7 Energy Modeling

The potential energy savings methods discussed in this research require and energy model. Using energy analysis, the tractive power required for the motion of the vehicle is found. The tractive power in kW is represented below.

$$P_{tr} = F_T v \tag{1.13}$$

v is the vehicle velocity in m/s and F_T is the tractive force in kN. By integrating the tractive power, the total tractive energy in kJ is evaluated as seen below.

$$E_{tr} = \int_{t_0}^{t_f} P_{tr} dt \tag{1.14}$$

t_0 is the start time, t_f is the final time, andP_{tr} is the tractive power. When $F_T > 0$, the energy required to meet driver demand is propel energy. When $F_T < 0$, the energy required to bake the vehicle is potential energy to be regained through regenerative braking. Energy is lost in ICE vehicles through friction braking. However, in both hybrids and battery electric vehicles, some of that braking energy can be regained by the system. When $F_T = 0$ the vehicle is in a coasting situation. In this situation, the vehicle will slow down by the motion resistant forces acting on the vehicle until a speed of zero is reached.

Energy consumption is represented as the amount of energy usage per unit distance (mi). This paper address how a Signalized Intersection Control Strategy can save energy at and nearing controlled intersections. This paper does not look at the effects vehicle powertrain efficiencies have on fuel consumption and instead look to limiting the total axle work to travel a given distance.

Chapter 2

Eco Adaptive Cruise Controller

The Signalized Intersection Control Strategy utilizes an Eco ACC MPC system developed by Tim Ryan [1]. Through cooperative action the Signalized Intersection Control Strategy was integrated into the Eco ACC MPC to ensure robustness and safety of the system. The following sections discuss the constraints, development, and creation of the Eco Adaptive Cruise Control MPC system.

2.1 Rideability

One of HEVT's main challenges is maintaining rideability and safety while increasing fuel economy. Rideability is a combination of the responsiveness of a vehicle, smoothness, and the rider's comfort [20]. Acceleration and jerk of a vehicle are used to determine the associated comfort level. Vehicle acceleration is represented by the rate of change in velocity and vehicle jerk is represented by the rate of change in acceleration.

Acceleration magnitudes begin to make a rider uncomfortable at a value 2 m/s^2 where as jerk begins to to make a rider uncomfortable at a value of 0.9 m/s^3 [20]. The ISO standard for for full range ACC is ISO22179. This states that at lower speeds, greater values for jerk and acceleration are acceptable. Therefor, at slower speeds, heavy braking events are more tolerable than at faster speeds due to braking power limits. The usable limits are described in the intelligent machines handbook [22].

2.2 Acceleration Request Cruise Control

To represent the overall architecture of any vehicle, an acceleration request cruise controller is developed. The adaptive cruise controller has an acceleration request cruise controller mode which utilizes the lower level controller to meet acceleration requests. The vehicle dynamics above are utilized to display a system that is controlled by an acceleration request, $u(t)$, which contains a time delay. The added time delay is used to represent road load parameters and delays in powertrain responses. The acceleration dynamics can be seen below.

$$\tau \frac{d\ddot{s}(t)}{dt} + \ddot{s}(t) = u(t) \tag{2.1}$$

τ is the time constant, $s(t)$ is the position of the Ego vehicle, $\dot{s}(t)$ is the Ego vehicle velocity, and $\ddot{s}(t)$ is the Ego vehicle acceleration. The acceleration request the vehicle is attempting to reach is represented by $u(t)$. The added time delay due to low level controllers is represented by τ [4]. Eq. 2.1 is amended to represent the new first order equations seen below.

$$\dot{x}_1(t) = x_2(t) \tag{2.2}$$

$$\dot{x}_2(t) = -\frac{1}{\tau}x_2(t) + \frac{1}{\tau}u(t) \tag{2.3}$$

$u(t)$ is the acceleration request, $x_2(t)$ is the vehicle acceleration, and $x_1(t)$ is the vehicle velocity. The state space representation of the dynamic equations is seen below.

$$\overbrace{\begin{bmatrix}\dot{x}_1(t)\\ \dot{x}_2(t)\end{bmatrix}}^{\dot{x}(t)} = \overbrace{\begin{bmatrix}0 & 1\\ 0 & -\frac{1}{\tau}\end{bmatrix}}^{A}\overbrace{\begin{bmatrix}x_1(t)\\ x_2(t)\end{bmatrix}}^{x(t)} + \overbrace{\begin{bmatrix}0\\ \frac{1}{\tau}\end{bmatrix}}^{B}u(t) \tag{2.4}$$

$$y(t) = \overbrace{\begin{bmatrix}1 & 0\end{bmatrix}}^{C}\begin{bmatrix}x_1(t)\\ x_2(t)\end{bmatrix}$$

Where the A and B represent the plant matrices and C is the output matrix. The intention is to find the acceleration request using a Linear Quadratic Integrator. By integrating the difference between the output $y(t)$ and the reference trajectory $r(t)$ an error state can be defined. The error state is defined below with the goal of driving the error to zero.

$$e(t) = \int_{t_0}^{t} (r(\tau) - y(\tau))d\tau \tag{2.5}$$

t_0 is the start time with t representing current simulation time. A modified system is considered with the objective of changing the acceleration request $u(t)$ to accurately track the reference trajectory $r(t)$. The modified state space equation is shown below.

$$\overbrace{\begin{bmatrix}\dot{x}(t)\\ \dot{e}(t)\end{bmatrix}}^{\dot{x}_{mod}} = \overbrace{\begin{bmatrix}A & 0\\ -C & 0\end{bmatrix}}^{A_{mod}} \overbrace{\begin{bmatrix}x(t)\\ e(t)\end{bmatrix}}^{x_{mod}(t)} + \overbrace{\begin{bmatrix}B\\ 0\end{bmatrix}}^{B_{mod}} u(t) + \overbrace{\begin{bmatrix}0\\ I\end{bmatrix}}^{B_r} r(t) \tag{2.6}$$

$$y(t) = \overbrace{\begin{bmatrix}C & 0\end{bmatrix}}^{C_{mod}} \begin{bmatrix}x(t)\\ e(t)\end{bmatrix}$$

x_{mod} is the modified state vector and A_{mod}, B_{mod}, and C_{mod} are the modified state matrices. The LQI controller will now follow a given reference trajectory. Optimization can be achieved by minimizing the cost function, $J(u)$, defined below.

$$J(u) = \int_0^\infty (x_{mod}^T Q x_{mod} + u^T R u) dt \tag{2.7}$$

The states and control inputs utilize the Q and R matrices for weighting. To get the desired perforce from the system, proper selection of Q and R is important. The cost matrices are seen below.

$$Q = \begin{bmatrix}q_1 & 0 & 0\\ 0 & q_2 & 0\\ 0 & 0 & q_3\end{bmatrix} \tag{2.8}$$

$$R = r_1 \tag{2.9}$$

Where q_1, q_2, q_3 and r_1 are scalar values greater than zero. Through the individual tuning of Q and R, the desire response is achieved. After tuning, a slower response was developed to further minimize the impact on acceleration and jerk for the vehicle. The final weights and variables are summarized in Table 2.1.

Table 2.1: Cruise Control Tuning Parameters

Parameter		
Time Delay	τ	.5
State Weights:	q_1	10^3
	q_2	0.1
	q_3	10^2
Control Weight:	r	10^4

To test this controller, a jerk limited reference trajectory was created. The trajectory is created by a piecewise continuous function. The acceleration request cruise controller

is successfully able to converge the set speed with limited acceleration and jerk. This can be seen below in Figure 2.1. The controller response is slow due to controller gains. This indented function will help lower magnitudes of acceleration and jerk.

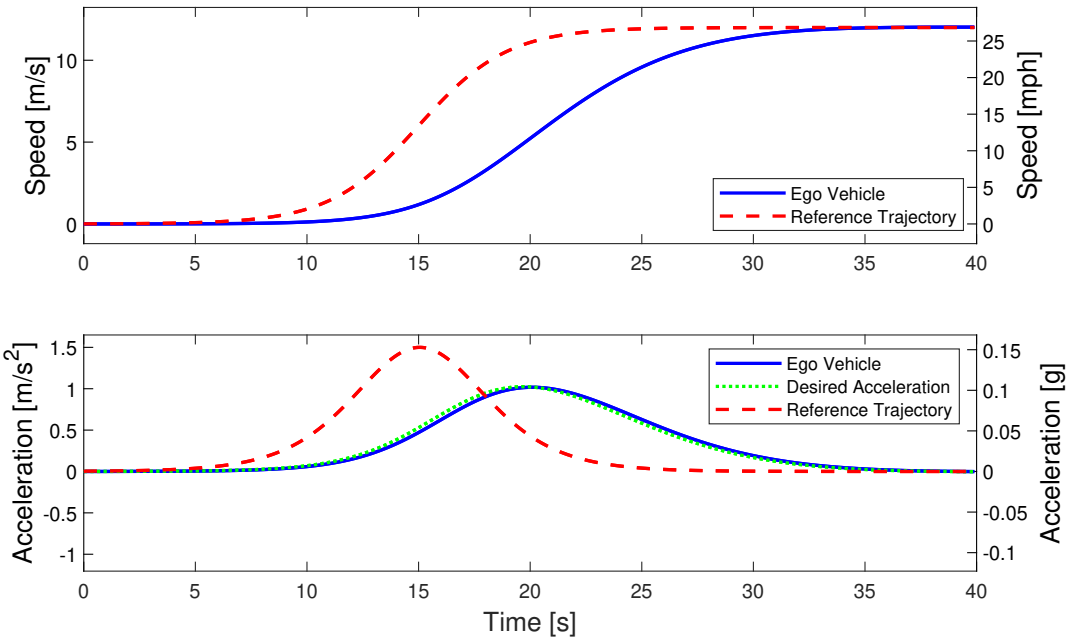

Figure 2.1: Acceleration Request Cruise Controller Response to Peicewise Reference Trajectory

The controller was put through additional testing to ensure its validity and for the purposes of this research is assumed to be functioning as intended. Overall, the acceleration request cruise controller works well to converge the error in velocity to zero.

2.3 Headway Control

After the development of a functioning acceleration request cruise controller, the next step in the creation of an Eco ACC MPC system is an appropriate headway control system that manages range and range rate of the Ego vehicle to the nearest object. The reliability of the headway controller is important when ensuring safety and accuracy of the system, especially when braking. In travel, the adaptive cruise control system switches between headway and cruise control modes when appropriate.

A headway controller works by regulating the distance and velocity of the Ego vehicle as it follows a lead vehicle. The Ego vehicle utilizes radar and visual sensors to track objects

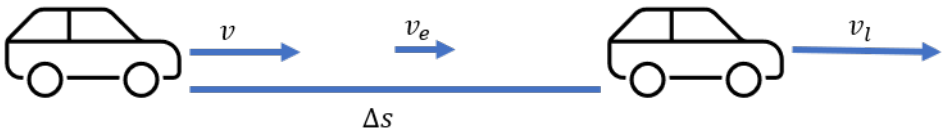

Figure 2.2: Headway Control Between Two Vehicles.

through the CAVs supervisory controller. A model of the lead and Ego vehicle is shown in Figure 2.2. The Ego vehicle motion is described by Equation 2.1.

After substituting $a(t)$ into Eq. 2.1, the dynamics are seen below. τ set at 0.5 seconds and $\ddot{x}(t)$ refers to the vehicle acceleration, $a(t)$.

$$\tau \frac{da(t)}{dt} + a(t) = u(t) \tag{2.10}$$

Utilizing a forward difference equation, the system can be re-written in order to calculate the next acceleration of the vehicle utilizing τ, T_s sampling time, and the current vehicle acceleration.

$$a(k+1) = (1 - \frac{T_s}{\tau})a(k) + \frac{T_s}{\tau}u(k) \tag{2.11}$$

Using $a(k)$ and $u(k)$, the next time step acceleration, $a(k+1)$, is found. The velocity equation is solved in a similar manner using the current acceleration as shown in Eq. 2.12.

$$v(k+1) = v(k) + T_s a(k) \tag{2.12}$$

Based on $a(k)$ and $v(k)$, the next time step velocity, $v(k+1)$, is found. The next important equation is the calculation of the future time step of longitudinal jerk. The final equation is shown in Eq. 2.13.

$$j(k+1) = -\frac{a(k)}{\tau} + \frac{u(k)}{\tau} \tag{2.13}$$

Using $a(k)$ and $u(k)$, the next time step jerk, $j(k+1)$, is found. The forward facing cameras and radar sensors report the difference in vehicle velocities as a rate of change in distance between lead and Ego vehicle. By plugging Eq. 2.12 into Eq. 2.14, Eq. 2.15 is found.

$$v_e(t) = v_l(t) - v(t) \tag{2.14}$$

$$v_e(k+1) = v_e(k) - T_s a(k) + T_s a_l(k) \tag{2.15}$$

Utilizing the current speed and acceleration, the next time step difference in speeds, $v_e(k+1)$, is found. The last state is represented by the relative distance between the Ego and lead vehicles. The relative distance equation is defined below.

$$\Delta s(t) = s_l(t) - s(t) \tag{2.16}$$

With the difference equation being seen below.

$$\Delta s(k+1) = \Delta s(k) + T_s v_e(k) - \frac{1}{2}T_s^2 a(k) + \frac{1}{2}T_s^2 a_l(k) \tag{2.17}$$

The next time step relative distance, $\Delta s(k+1)$, is based on the current states.

The motion between the Ego and lead vehicle are represented by the system of equations seen below.

$$\begin{aligned}
\Delta s(k+1) &= \Delta s(k) + T_s V_e(k) - \frac{1}{2}T_s^2 a(k) + \frac{1}{2}T_s^2 a_l(k) \\
v(k+1) &= v(k) + T_s a(k) \\
v_e(k+1) &= v_e(k) - T_s a(k) + T_s a_l(k) \\
a(k+1) &= (1 - \frac{T_s}{\tau})a(k) + \frac{T_s}{\tau}u(k) \\
j(k+1) &= -\frac{a(k)}{\tau} + \frac{u(k)}{\tau}
\end{aligned}$$

$k+1$ is the future time sample and $k(s)$ is the current time sample.

The requested acceleration is the manipulated variable in this system while the lead vehicle acceleration is a known disturbance. Luo's MPC paper describes the main construction of the controller dynamics discussed [14] [13] with the final state space representation being shown below.

$$x(k+1) = Ax(k) + Bu(k) + Gw(k) \tag{2.18}$$

$$y(k) = Cx(k) - Z \tag{2.19}$$

With the state matrix's taking the forms seen below.

$$A = \begin{bmatrix} 1 & 0 & T_s & -\frac{1}{2}T_s^2 & 0 \\ 0 & 1 & 0 & T_s & 0 \\ 0 & 0 & 1 & -T_s & 0 \\ 0 & 0 & 0 & 1 - \frac{T_s}{\tau} & 0 \\ 0 & 0 & 0 & -\frac{1}{\tau} & 0 \end{bmatrix}, \quad B = \begin{bmatrix} 0 \\ 0 \\ 0 \\ \frac{T_s}{\tau} \\ \frac{1}{\tau} \end{bmatrix}, \quad G = \begin{bmatrix} \frac{1}{2}T_s^2 \\ 0 \\ T_s \\ 0 \\ 0 \end{bmatrix},$$

$$C = \begin{bmatrix} 1 & -t_h & 0 & 0 & 0 \\ 0 & 1 & 0 & 0 & 0 \\ 0 & 0 & 1 & 0 & 0 \\ 0 & 0 & 0 & 1 & 0 \\ 0 & 0 & 0 & 0 & 1 \end{bmatrix}, \text{ and } Z = \begin{bmatrix} d_0 \\ 0 \\ 0 \\ 0 \\ 0 \end{bmatrix}$$

Conditions that cannot be violated by the system to ensure safety are referred to as hard constraints. When properly used in headway control, a hard constraint will ensure no collision with a preceding object happens. The hard distance constraint is seen below where $s_{critical}$ is the minimum safe following distance.

$$\Delta s \geq s_{critical} \tag{2.20}$$

Some constraints were added to ensure better rideability while keeping the vehicle within it's a realistic power limits. The following are also defined as hard constraints.

$$v_{min} \leq v(k) \leq v_{max} \tag{2.21}$$
$$a_{min} \leq a(k) \leq a_{max} \tag{2.22}$$
$$u_{min} \leq u(k) \leq u_{max} \tag{2.23}$$

However, jerk is a soft constraint and needs be minimized. The jerk limits are defined below.

$$j_{min} \leq j(k) \leq j_{max} \tag{2.24}$$

The MATLAB MPC toolbox is used to create the MPC controller and it is assumed that the logic of the MATLAB commands function as intended. The control and prediction

horizon matrices within toolbox are used for tuning. For real time calculations, these tuning matrices should be limited to reduce computational needs.

The MPC algorithm gives the creator a robust tuning situation where weights, prediction horizon, and control horizon can all be adjusted. The first command utilized from MATLAB is seen below.

$$\text{mpcobj} = \text{mpc(plant,ts,P,M,W,MV,OV,DV)}$$

This command initializes the MPC object utilizing the "plant dynamics, prediction horizon (P), control horizon (M), weights (W), output variables (OV), and manipulated variables (MV)" [15]. Using the manipulated and output variables, the minimums, maximums, hard and soft constraints can be assigned to the MPC object. The next MATLAB command runs the optimization problem known as quadratic programming (QP) which utilizes the reference trajectory and assigned constraints.

$$\text{mv} = \text{mpcmove(MPCobj,xc,ym,r,w)}$$

Based on the MPC model, known disturbance (w), and reference trajectory (y_{ref}), the desired control input based on the MPC model can be found. The tuning process is based on the plant dynamics Eq. 2.18 and measured disturbances with the weight matrix being defined below.

$$Q = diag(\begin{bmatrix} q_1 & q_2 & \dots & q_N \end{bmatrix})$$

All q_i are greater than zero defining Q as a positive definite matrix. The first entry refers to the first output variable and the final entry refers to the final output variable (vector notation). After a lengthy tuning process, the final weights for all aspects of the MPC controller in MATLAB were established and are displayed in Table 2.2. The parameters and constraints of the MPC system during simulation are displayed in Table 2.3.

Through simulations, the validity of the headway controller is confirmed and assumed to be functioning correctly for the purposes of this research. A switching algorithm is used to determine when the vehicle should be in regular cruise control mode vs headway control mode. The variables considered for this evaluation are time headway gap and relative vehicle speed. When the Ego vehicle is faster then the lead vehicle and within the vehicle gap, the headway controller is used. When the Ego vehicle is traveling slower than the lead vehicle, the Ego vehicle will use cruise control mode. The switch case is displayed in Table 2.4. The Adaptive Cruise Control Strategy displayed in this paper is derived from Ryan's work on Eco ACC MPC systems with minor modifications that will be discussed in the next chapter [1].

Table 2.2: MPC tuned parameters for headway control algorithm

Parameter		
Prediction Horizon	N_p	30
Control Horizon	N_c	3
Manipulated Variable Weight	MV	1
Manipulated Variable Rate Weight	$MVRate$	.01
Relative Distance Weight	q_1	1
Velocity Weight	q_2	0
Relative Velocity Weight	q_3	3
Acceleration Weight	q_4	1
Jerk Weight	q_5	1

Table 2.3: Variable consideration during simulation

Parameter		Units	Min	Max
Relative Distance	Δs	m	5	∞
Velocity	v	m/s	0	35
Relative Velocity	v_e	m/s	$-\infty$	∞
Acceleration ($v < 5$)	a	m/s^2	-5	2
Acceleration ($5 \leq v < 20$)	a	m/s^2	$-5.5 + v/10$	2
Acceleration ($v \geq 20$)	a	m/s^2	-3.5	2
Jerk	j	m/s^3	-2	0.9

Table 2.4: Conditions for adaptive cruise control

State	Requirement
Cruise Control	$V_{lead} > V_{ego}$ when $V_{lead} > V_{set}$
	OR
	$\Delta s \geq v_{ego} * (t_h + 4.5) + d_o$
Headway Control	**Otherwise**

Chapter 3

Signalized Intersection Control Strategy

Various methods of intersection speed control have been discussed in this paper thus far. One of the methods is using an all encompassing MPC system that dealt with lead vehicles as well as impending intersections [21]. Another took the form of two separate MPC systems, one for headway control and another for intersection control [6]. In this research, another method was explored and tested. The next sections will cover the development of the Signalized Intersection Control Strategy.

3.1 Control Strategy Development

One of the major limitations of a Model Predictive Controller is its ability to be run in real time [9]. By running a complex algorithm with bounding constraints, an MPC system is able to produce optimized results. Better results are obtained by having larger control and predictions horizons. However, this drastically increases the complexity of the system leading to longer run times. Rather than adding more complexity to an existing tuned Eco ACC system, a background operation was developed that would update the set speed of the controller every time iteration.

Prior to any controller integration, the base Signalized Intersection Control Strategy was developed in MATLAB on its own. This allowed for development and debugging to be performed without the added complexity of the ACC system. Utilizing the working principles of the Green Light Optimized Speed Advisory system, the development and testing was focused around a single connected intersection at one time [23]. Narrowing the scope to a single intersection approach allows for a deeper look into the decisions being made around the intersection. Early in the development process a decision was made that would segregate the control strategy into different sections. The first section being how the vehicle is controlled

without needing to come to a complete stop. The second is how the braking of the vehicle is handled when a complete stop is necessary.

3.1.1 Speed Control

The first step in creating the control strategy is the knowledge of what information is available to a vehicle via V2I short range communication. The terms utilized in research and industry are Signal Phase and Timing (SPaT) data and MAP data. SPaT data represents the current phase of the traffic light (green or red) as well as the amount of time remaining before a phase change (timing). MAP data is utilized along with the vehicles current geospacial position to determine the current distance the vehicle is from the intersection stop line. For the purposes of this research, these signals are assumed to be correct and each simulation will begin when both signals are received by the Ego vehicle. This means the control strategy will have several inputs and a single output being the next set speed of the system. The inputs are as follows:

- Current phase of the light.
- Amount of time remaining until phase change.
- Distance to the intersection stop line.
- Current vehicle speed.
- Current set speed.

With the inputs and outputs noted, the decisions made throughout the control strategy can be discussed. Firstly, there are three main points being checked through the duration of each simulation. These are as follows:

- Has a full stop been requested?
- Has the light changed from its initial phase?
- Is the current phase green?

The first check made by the system is whether the stop request has been initiated while also making sure the light phase has not changed from its starting phase. Decisions in the strategy are made based on a single traffic light which once changes from its initial phase is not considered to change any further. This is because at this point the Ego vehicle has either passed through the light or will when the light phase turns green. If the stop condition has not been initiated and the light phase has not changed, then the next data being checked is the current phase of the light. There are two different paths utilising this information.

A green light velocity path and a red light velocity path. Both paths utilize Eq. 3.1 to determine the critical velocity that gets the vehicle to the stop line when the phase changes.

$$Vel_{g/r} = \frac{inDist}{tLight} \tag{3.1}$$

Where $Vel_{g/r}$ is the critical velocity to the stop light at the phase change, $inDist$ is the distance to the stop line, and $tLight$ is the amount of time remaining until the next phase change.

With the critical velocity calculated for both the red phase and green phase depending on the simulation, each path makes different comparisons. If the initial phase is green, the vehicle can either maintain its current speed, or accelerate a little to make the light before a phase change. If neither is possible the vehicle must come to a stop anticipating the red phase. However, if the starting phase is red, the vehicle can either maintain speed, decelerate a set amount determined by the control strategy, or the vehicle must come to a stop anticipating the phase will be red upon reaching the stop line. Both of these scenarios can be seen below. If the first condition is not met then the equation below is checked next until completion.

$$Vel_g <= V_{actual} + 2 \; and \; Vel_g > V_{actual} \; --yes-> \; vset = Vel_g \tag{3.2}$$

$$Vel_g <= V_{actual} \; --yes-> \; vset = V_{actual} \tag{3.3}$$

Where V_{actual} is the current velocity of the Ego vehicle, and vset is the next set speed output of the control strategy. If the first condition is not met then the equation below is checked next. If that condition is also not satisfied then the stop command is initiated.

$$Vel_r <= vset \; --yes-> \; vset = vset \tag{3.4}$$

$$Vel_r <= V_{original} - 4.5 \; --yes-> \; Stop\,Command\,Initiated \tag{3.5}$$

$$vset = Vel_r \tag{3.6}$$

Where V_{actual} is the current velocity of the Ego vehicle, and vset is the next set speed output of the control strategy. Vel_r is compared to $V_{original} - 4.5$ to set the minimum speed the system can decelerate to without needing to perform a full brake maneuver. Similarly, if the first condition is not met then the equation below is checked. If that one too is not met then $vset$ is updated to the critical speed Vel_r. This portion of the Signalized Intersection Control Strategy can be seen in Fig. 3.1.

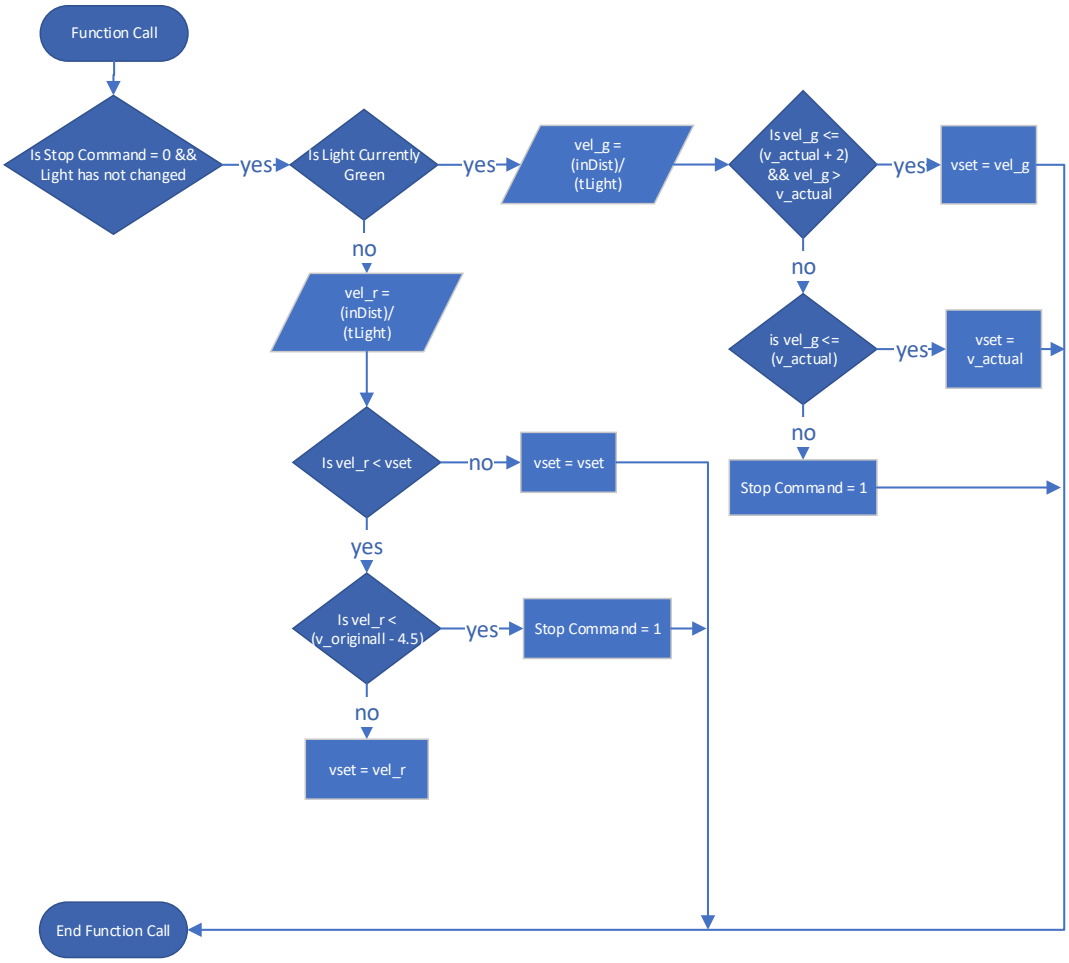

Figure 3.1: Traffic Light Logic Diagram Part 1

The next check made by the system is whether the stop request has been initiated while also checking that the light has changed phases. If the stop request has not been initiated and the light has changed phases, then the Ego vehicle has passed through the light without the need to come to a complete stop. There are two cases where this will happen. If the vehicle slowed down during a red phase to pass through the intersection; or, if the vehicle accelerated to pass through the intersection during a green phase. This section of the control strategy is designed to bring the vehicle back to its original set speed.

If neither of the previous checks caused the system to loop in their respective sections of the control strategy, the stop command has been initiated. The control strategy then verifies if the stop command has been initiated while the current set speed is non-zero. If so, the system will begin its braking algorithm bring the vehicle to a stop in an energy efficient manner. This will be discusses in detail in the next section of this paper. However, if the stop

command has been initiated and the current set speed is zero, the next set speed ($vset$) will again be updated with a value of zero. This portion of the Signalized Intersection Control Strategy can be seen below represented by a Logic Diagram in Fig. 3.2. The variables in this figure will also be discussed in the next section.

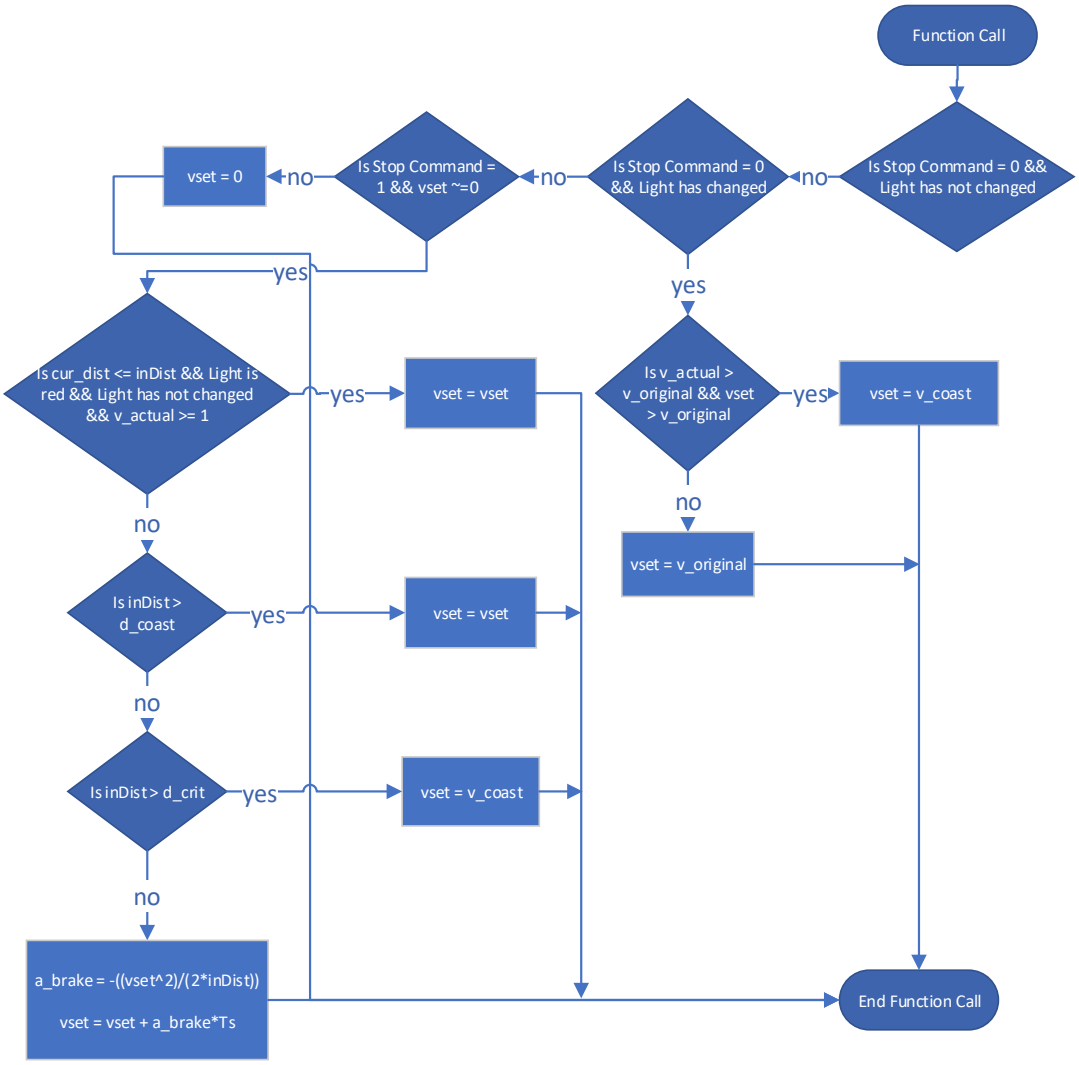

Figure 3.2: Traffic Light Logic Diagram Part 2

3.1.2 Vehicle Braking

Once the Signalized Intersection Control Strategy has decided the Ego vehicle needs to make a complete stop, the control strategy enters the braking section of its methodology seen in

Fig 3.2. In order to bring the Ego vehicle to a stop in an efficient manner based on traffic signal information, it is desirable for the vehicle to coast when possible. When coasting, a vehicle is utilizing zero tractive energy to slow the vehicle down.

The partial differential equation below represents the acceleration of a vehicle with zero grade.

$$\frac{dv_c}{dt} = -\frac{(C_{r,0} + C_{r,1}v_c)mg + \frac{1}{2}\rho A_f C_D v_c^2}{\delta_I m} \tag{3.7}$$

The coasting velocity is represented by v_c. Eq. 3.7 is represented below for easier implementation and legibility.

$$\frac{dv_c}{dt} = -\alpha_1^2 - \alpha_2^2 v_c - \beta^2 v_c^2 \tag{3.8}$$

$$\alpha_1 = \sqrt{C_{r,0}g/\delta_I}$$
$$\alpha_2 = \sqrt{C_{r,1}g/\delta_I}$$
$$\beta = \sqrt{\frac{\rho A_f C_D}{2\delta_I m}}$$

Through the integration of Eq. 3.8, the coasting velocity, $v_c(t)$, is found.

$$v_c(t) = \frac{-\left(\alpha_2^2 - tan\Big(atan\Big(\frac{\alpha_2^2 + 2v_0\beta^2}{\sqrt{-\alpha_2^4 + 4\alpha_1^2\beta^2}}\Big) - t * \frac{\sqrt{4 * \alpha_1^2 * \beta^2 - \alpha_2^4}}{2}\Big)\sqrt{4\alpha_1^2\beta^2 - \alpha_2^4}}{2\beta^2} \tag{3.9}$$

With v_0 being the initial velocity.

Using Eq. 3.9 a coasting look-up table is created in order to allow the Signalized Intersection Control Strategy to make set speed updates that follow a coasting profile. Once below $5m/s$ however, the deceleration is fixed at $-0.5m/s^2$ to improve transition situations. Fig. 3.3 displays a velocity coasting profile, distance coasting profile, and a combined distance vs velocity profile used to determine the next set speed output from the control strategy. The green region represents a constant velocity region. In this region, the Ego vehicle is far enough away from the stop line of the intersection to maintain its current speed until it crosses into the blue region. The blue region is the coasting region. In this region, the current speed and distance from the stop line permit the vehicle to coast towards the intersection until the distance and velocity data show a cross into the red region. This region is referred to as the critical braking region. Once into this region the Ego vehicle must perform active braking to ensure it does not run a red light. The beginning of the critical braking line is a constant deceleration of $-0.5m/s^2$ to match up with the lower speed section of the

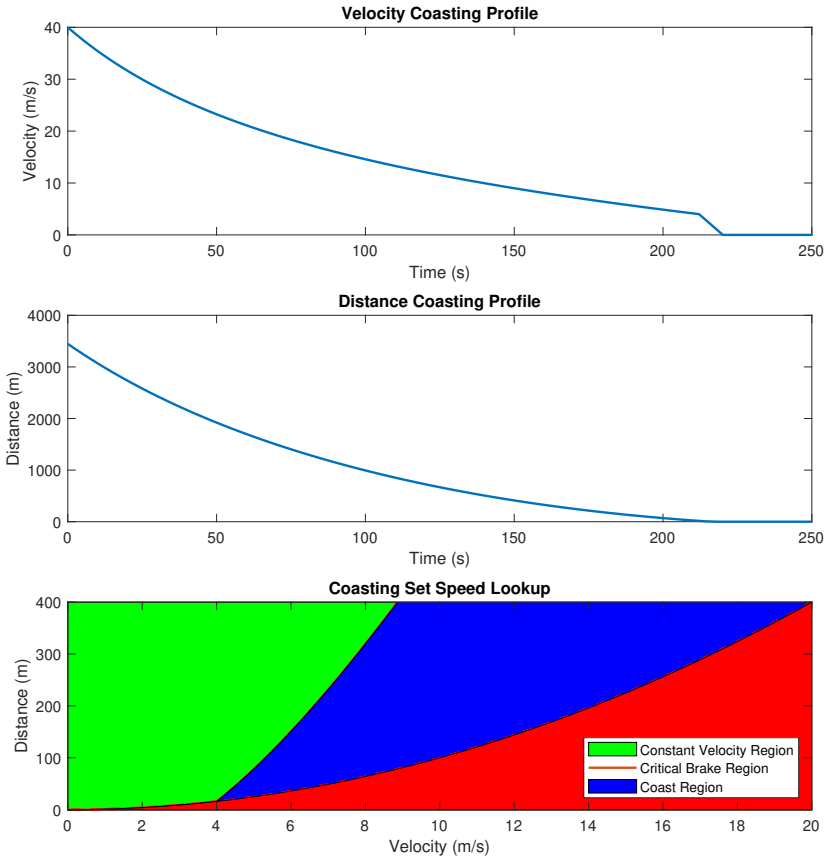

Figure 3.3: Vehicle Brake Lookup Table

coasting profile. While this is a conservative deceleration value, it ensures the Ego vehicle maintains its rideability standards mentioned earlier. The active braking section utilizes Eq. 3.10 below. The final equation is derived from the first with the assumption that the final vehicle velocity $V_f^2 = 0$.

$$V_f^2 - V_0^2 = 2 * a * d \tag{3.10}$$

$$a = -\frac{V_0^2}{2 * d} \tag{3.11}$$

Where a is the Ego vehicle acceleration, V_0 is the Ego vehicle current set speed, and d is how far the Ego vehicle is currently from the intersection stop line. The acceleration a shown above is then multiplied by the system simulation time step $T_s = 0.1s$, and then added to the current set speed of the system, to find the next set speed output from the control strategy.

There is a special case in the braking section of the control strategy that does not bring the Ego vehicle to a stop. Rather, the vehicle is slowed down from either coasting or active braking until the current speed of the vehicle will allow an intersection crossing during a green light. All brake to stop maneuvers are back calculated from how far the Ego vehicle is from the intersection stop line, leading to a distance based speed update strategy. As seen in Fig. 3.1, the control strategy only allows the Ego vehicle to decelerate to a speed no lower then 4.5 m/s slower than the original set speed, or about $10mph$ slower. This limit is set for the safety of the Ego vehicle and any potential following vehicles. However, this means that if the vehicle requests a full stop and performs either coasting or active braking, there can come a point when the current speed will allow the Ego vehicle to pass through the intersection during a green phase. Rather than having the Ego vehicle continue braking only to accelerate again when the light phase changes, another check is performed. When the vehicle is braking for a stop, Eq. 3.12 is used as a comparison to the current distance the vehicle is from the intersection stop line. The variables in the equation match the variables shown in the Logic Diagram above.

$$Cur_{dist} = V_{actual} * tLight \tag{3.12}$$

Cur_{dist} is the current distance the Ego vehicle can travel with the current speed and time remaining until phase change, V_{actual} is the current vehicle speed, and $tLight$ is the amount of time remaining until the next phase change. When Cur_{dist} becomes smaller then the distance between the vehicle and stop line ($inDist$), the next $vset$ output is set to the current vehicle set speed. All of this is shown graphically above in Fig. 3.2.

While the control strategy has been created, it still needs to be vetted to ensure the state flow is following the intended path. A few simple test scenarios were created to see how the control strategy responded. Fig. 3.4 represents one of these early test cases to validate the Signalized Intersection Control Strategy without any additional controllers. In this scenario, the Ego vehicle receives SPaT and MAP data when $200m$ away from the intersection stop line. The light phase is currently red and will turn green after $30s$. The control strategy determines that a full stop is required to not pass through the intersection on a red phase. The set speed becomes zero as the Ego vehicle gets to the stop line. Once the phase turns green, the set speed is updated back to the original set speed. This simple scenario demonstrates the control strategies ability to successfully update the set speed of the system.

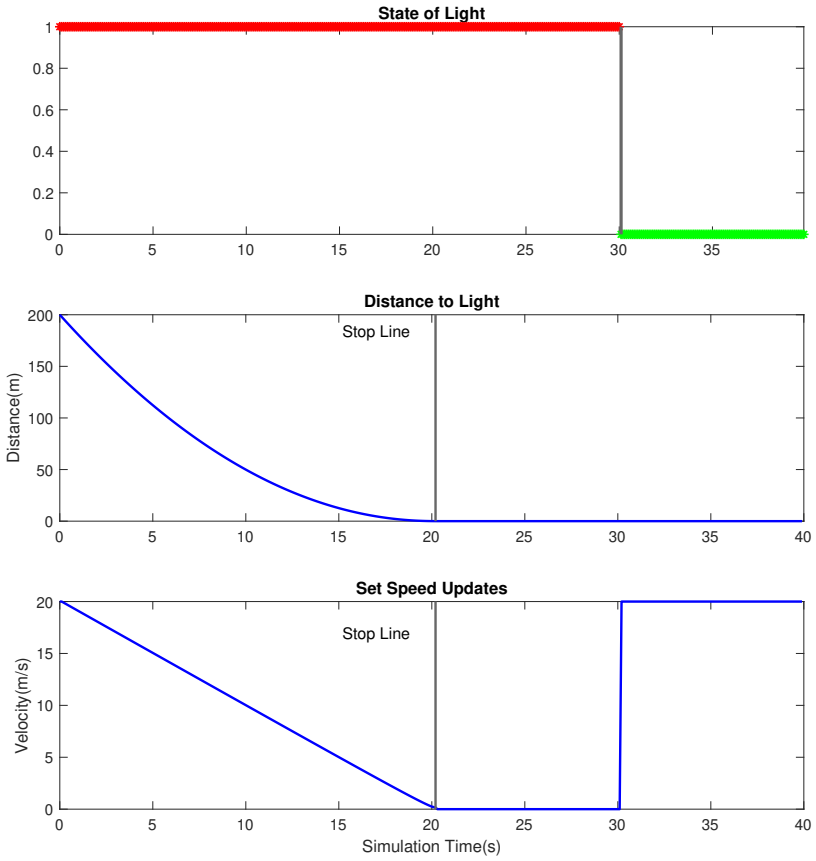

Figure 3.4: Sample Simulation without Vehicle Controller Implemented

3.2 Controller Integration and Implementation

The Signalized Intersection Control Strategy has been tested and verified without the use of additional controllers. The last step is the integration of the control strategy into the Eco Adaptive Cruise Controller [1]. Once integrated, the control strategy will be thoroughly tested with the vehicle controllers, ACC and regular cruise control, to ensure it does not take away from the safety and rideability standards the Eco ACC was developed around.

The Signalized Intersection Control Strategy was converted into a callable function to be used by the Eco ACC system. The inputs into this function call are current set speed, current vehicle speed, original set speed, distance to stop line, current phase, and time remaining until phase change. The only output of this call function is the next time step set speed. Utilizing this method allows the integration of the two systems with only minor changes to the Eco ACC. One of the more significant changes to the vehicle control is the utilization of the MPC system for accurate braking. Switching logic is required when implementing multiple controllers. Multi-threading is the operation by which this transition occurs [16]. The Signalized Intersection Control Strategy does not directly utilize the MPC portion of the cruise controller. However, when the Signalized Intersection Control Strategy has determined a full stop necessary, then the MPC portion is used to safely bring the Ego vehicle to a stop at the intersection stop line. This is accomplished by comparing the distances between the Ego vehicle and both the stop line and current lead vehicle. This comparison is checked every time step to ensure safety of the Ego vehicle. The function created is set to be called every iteration of the simulation (Ts) to more closely represent the Ego vehicle receiving sensor fusion information every time sample, along with SPaT and MAP data when applicable.

The combined Eco ACC with SPaT information system will be tested against an assumed uninformed driver in order to make compelling comparisons of energy consumption reduction. One method of simulating an uninformed driver is only allowing the vehicle to start a braking maneuver when the visual queue of a yellow light phase would be initiated. Similar to the informed system simulation, the uninformed system will utilize the MPC controller portion of the Eco ACC system to bring the vehicle to a stop at the intersection stop line. Once the signal for the yellow light has been initiated, the MPC states are updated with the relative distance to the nearest object as the distance to the stop line and relative speed to nearest object as the negative of the current speed. The time at which the yellow light signal is initiated is found utilizing Eq. 3.13 seen below [10].

$$Y(v) = T_{pr} + \frac{V_a}{2d_r + 2gG_r} \tag{3.13}$$

$Y(v)$ is the yellow phase interval time, d_r is the deceleration rate (using $10ft/s$), g is the gravitational acceleration, G_r is the approach grade, T_{pr} is the driver reaction time (using $1s$), and V_a is the speed of the approaching vehicle ($vset$). All situations being studied in

this paper are absent of road grade. This leaves Eq. 3.13 to take the form seen below.

$$Y(v) = T_{pr} + \frac{V_a}{2d_r} \tag{3.14}$$

While this methodology will work when the initial phase in simulation is green, it will not make sense when an uninformed driver is approaching the intersection that is already red. In these instances, the distance the vehicle could travel, using Eq. 3.15, is used as the start of the uninformed vehicle braking maneuver. Meaning, when the uninformed driver is a distance D_{yellow} away from a red intersection, the vehicle will start its braking maneuver. This will keep the uninformed driver comparison consistent across all cases being observed.

$$D_{yellow} = V_{set} * Y(v) \tag{3.15}$$

Where D_{yellow} is the distance used for braking in the uninformed driver scenarios, V_{set} is the original vehicle set speed, and $Y(v)$ is the yellow phase interval time.

3.2.1 Test Conditions

Prior to testing, test conditions are created to explore the different modes of the control strategy. The descriptions of the tests are described below. These test are important when analysing the proper implementation of the control strategy and to further analyze energy consumption. In each test case, the Ego vehicle is equipped with the Signalized Intersection Control Strategy described in this paper along with the Eco ACC system [1].

Cases 1-6 will be compared to an assumed uninformed driver (vehicle does not have access to SPaT and MAP data).

1. **Simple Stop at a Red Light**
   The lead vehicle is not considered in this case. The Ego vehicle is at cruising speed some distance away from the signalized intersection. Upon receiving SPaT and MAP data the light is currently green but will turn red shortly. The vehicle is expected to come to a complete stop at the stop line.

2. **Simple Stop at a Red Light with Acceleration**
   The lead vehicle is not considered in this case. The Ego vehicle is at cruising speed some distance away from the signalized intersection. Upon receiving SPaT and MAP data the light is currently red and will turn green after some time. The vehicle is expected to come to a complete stop at the stop line and then accelerate to the original cruising speed once the light turns to green.

3. **Limited Acceleration to Pass Though the Light**
   The lead vehicle is not considered in this case. The Ego vehicle is at cruising speed some distance away from the signalized intersection. Upon receiving SPaT and MAP data the light is currently green and will turn red shortly. The vehicle is expected to speed up by a limited amount in order to pass through the intersection while the light is green.

4. **Limited Deceleration to a Constant Speed with Active Braking.**
   The lead vehicle is not considered in this case. The Ego vehicle is at cruising speed some distance away from the signalized intersection. Upon receiving SPaT and MAP data the light is currently red and will turn green after some time. The vehicle is expected to slow down to a constant speed. Then begin an intended full brake function but instead match a slightly lower constant speed to pass through the intersection just as the light changes to green.

5. **Limited Deceleration to a Constant Speed**
   The lead vehicle is not considered in this case. The Ego vehicle is at cruising speed some distance away from the signalized intersection. Upon receiving SPaT and MAP data the light is currently red and will turn green after some time. The vehicle is expected to slow down to a constant speed in order to pass through the light once it turns green.

6. **SPaT Data Received much Further Away**
   The lead vehicle is not considered in this case. The Ego vehicle is at cruising speed some distance away from the signalized intersection. Upon receiving SPaT and MAP data the light is currently red and will turn green after sometime. The vehicle is expected to slow down to a constant speed and then pass through the intersection once the light turns green. This case is designed to show the potential energy savings if accurate data can be received much further away from the intersection.

7. **Following a Vehicle to the Intersection**
   The lead vehicle is considered in this case. The Ego vehicle is at cruising speed some distance away from the signalized intersection with the lead vehicle traveling the same speed. Upon receiving SPaT and MAP data the light is currently green and will turn red shortly. The vehicle was anticipating being able to make the light by accelerating a small amount. However, due to the lead vehicle, the Ego vehicle is instead expected to come to a complete stop at the stop line.

8. **Vehicle Cut in Prior to the Stop Line**
   The lead vehicle is considered in this case. The Ego vehicle is at cruising speed some distance away from the signalized intersection with no lead vehicle currently in its path. Upon receiving SPaT and MAP data the light is currently green and will turn red after some time. The Ego vehicle is expecting the make the light without any changes in speed. However, the lead vehicle will cut in front of the Ego vehicle prior

to the intersection. The Ego vehicle is expected to come to a stop at the intersection stop line while maintaining a safe following distance.

3.2.2 Signalized Intersection Control Strategy Results

A majority of this analysis focuses on, propel/brake energy at the wheel, vehicle acceleration, vehicle jerk, and travel time. The vehicle acceleration and jerk are observed to ensure the rideability of the Ego vehicle once the control strategy has been implemented. One important point to note is that the specific SPaT and MAP data was derived in order to procure the case by case response from the Signalized Intersection Control Strategy and Eco ACC MPC system. The combination of SPaT and MAP data shown in the presented scenarios are not the only combination to procure the responses shown.

All energy comparison simulation results can be seen below in Table 3.1.

1. **Simple Stop at a Red Light**
   In the simulation, both the informed Ego vehicle and uninformed driver come to a complete stop at the intersection stop line. The Ego vehicle utilizes 6.6 Wh/mi while the uninformed driver utilizes 81 Wh/mi to traverse the same distance. The informed system shows a 92% decrease in propel energy consumption compared to the uninformed driver. The uninformed driver also experiences large jerk and acceleration sections compared to the informed system. The travel time for the informed system is 7 seconds longer in this case compared to the uninformed driver. This is because the informed system has prior knowledge that the intersection will not be passable during the current phase timing and begins braking early whereas the uninformed driver retains a constant speed until closer to the intersection which reduces travel time. The simulated plot for the informed system Fig. 3.5 can be seen below while the uniformed driver Fig. A.1 can be seen in the Appendix.

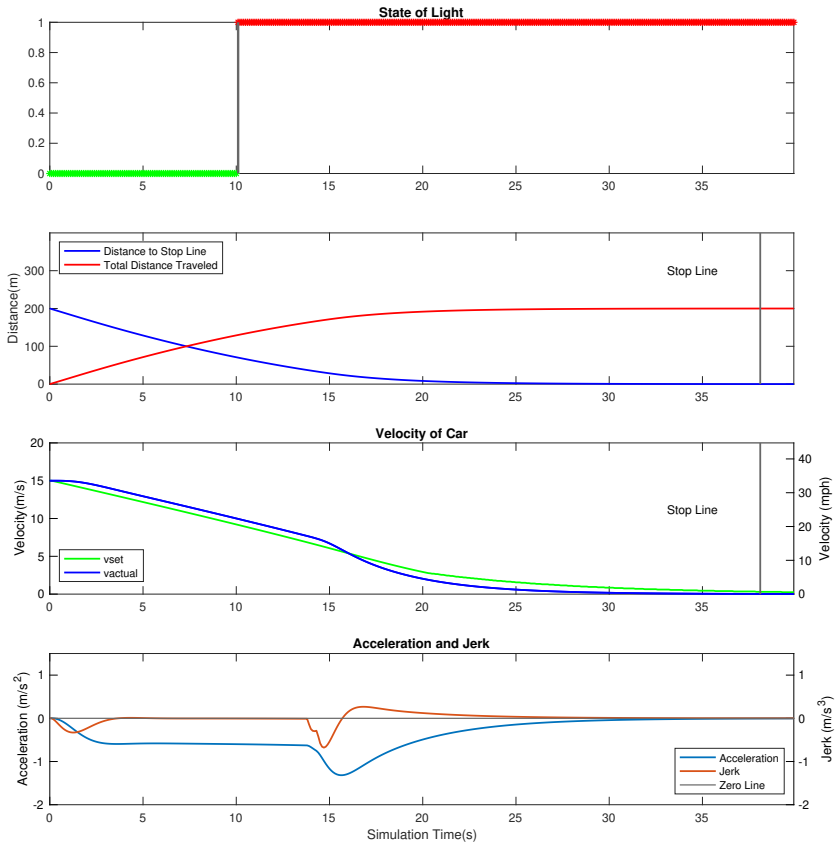

Figure 3.5: Case 1: Red Light Stop

2. **Simple Stop at a Red Light with Acceleration**
   In the simulation, both the informed Ego vehicle and uninformed driver come to a complete stop at the intersection stop line. They both then proceed back to their original set speed once the phase turns to green. The Ego vehicle utilizes 385 Wh/mi while the uninformed driver utilizes 433 Wh/mi to traverse the same distance. In this case the informed system shows a 11% decrease in propel energy consumption compared to the uninformed driver. The informed system takes an additional 5 seconds to traverse the same distance due to acceleration and jerk limits placed on the Eco ACC system. Fig. 3.6 displays the response of the informed system having access to SPaT and MAP data. Fig. A.2 demonstrates how an uninformed driver would traverse the same distance.

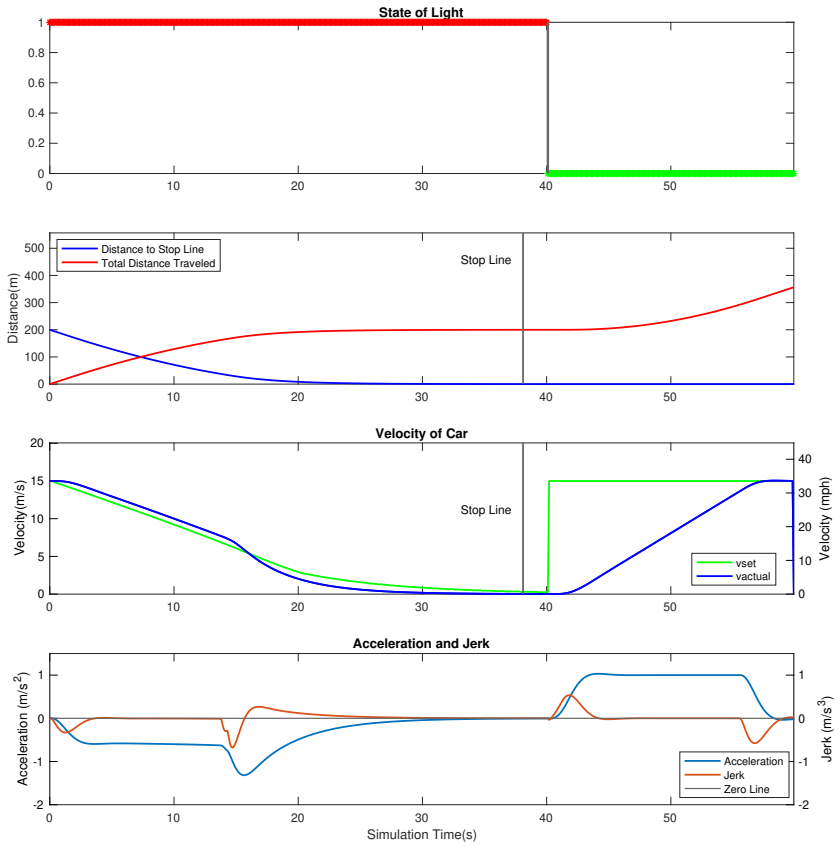

Figure 3.6: Case 2: Red Light Stop with Acceleration

3. **Limited Acceleration to Pass Though the Light**
   In the simulation, the informed system is able to speed up the Ego vehicle to a faster set speed in order to pass through the intersection during a green phase. The informed system then coasts back to the original set speed once through the intersection. The uninformed driver has to make a hard braking maneuver to not pass through the intersection during a red phase. The informed system utilizes 166 Wh/mi while the uninformed driver utilizes 256 Wh/mi to traverse the same distance. In this case the informed system demonstrates a 35% decrease in propel energy consumption compared to the uninformed driver. The informed system travels the simulated distance in 60 seconds while the uninformed driver takes 112 seconds due to a necessary traffic stop. Fig. 3.7 displays the informed system response while the uninformed driver's response can be seen in Fig. 3.8.

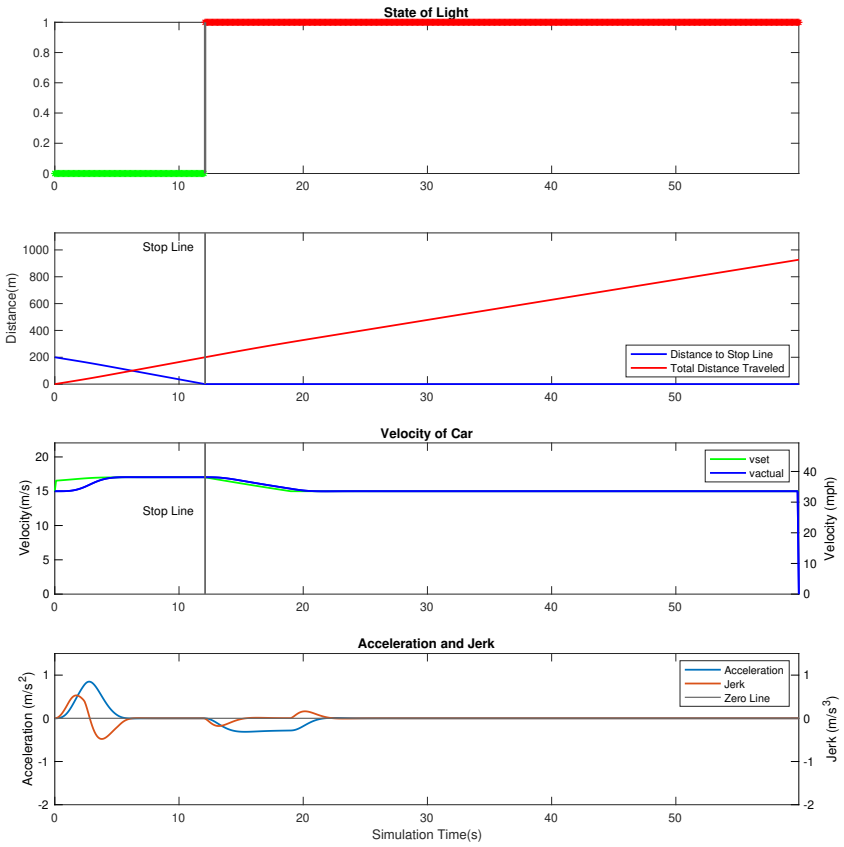

Figure 3.7: Case 3: Small Acceleration

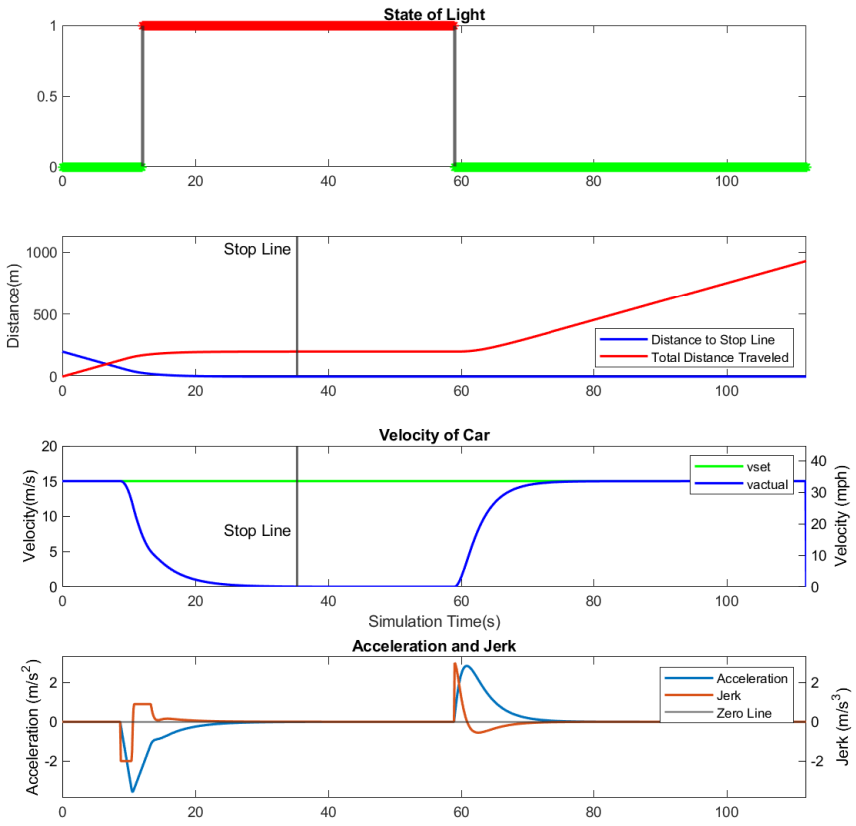

Figure 3.8: Case 3: Uninformed Driver

4. **Limited Deceleration to a Constant Speed with Active Braking.**
In the simulation, the informed system is able to slow down to a constant speed in order to pass through the intersection during a green phase rather than coming to a complete stop at the intersection stop line. Similar to the next case, the Signalized Intersection Control Strategy first attempts to slow the Ego vehicle down to a constant set speed in order to pass through the intersection at the green phase. However, the response of the Ego vehicle to the changing set speed is too slow which then requires the system to start a braking maneuver. During this braking maneuver, the distance the Ego vehicle could travel under its current speed and time remaining until phase change is compared to the distance remaining until the intersection stop line utilizing Eq. 3.12. Once these distances match, the control strategy keeps the current speed the same until the vehicle passes through the intersection as seen in Fig. 3.9. The uninformed driver is required to make a hard braking maneuver to not pass through the intersection during a red phase as seen in Fig. A.3. The informed system utilizes 271 Wh/mi while the

uninformed driver utilizes 365 Wh/mi to traverse the same distance. In this case the informed system demonstrates a 26% decrease in propel energy consumption compared to the uninformed driver. The uninformed driver only takes an additional two seconds to traverse the simulation distance compared to the informed system.

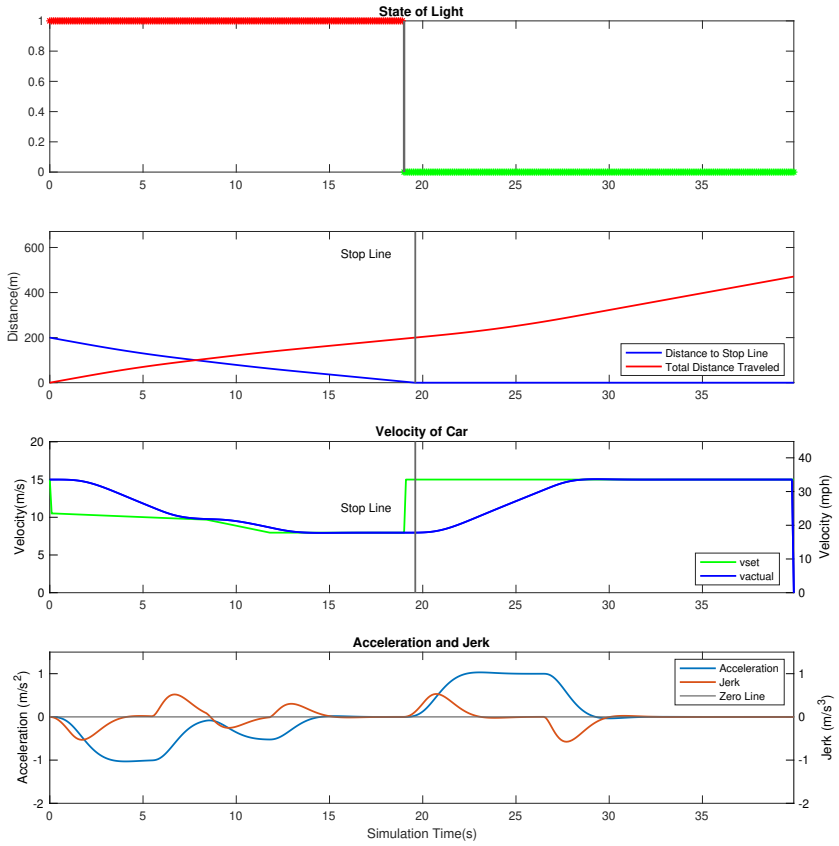

Figure 3.9: Case 4: Initial Small Deceleration to Active Braking

5. **Limited Deceleration to a Constant Speed**
   In the simulation, the informed system is able to slow down to a constant speed in order to pass through the intersection during a green phase. Once through the intersection the informed system drives the Ego vehicle back to the original set speed. The Ego vehicle observes minor acceleration and jerk regions in this simulation as the change in speed requested is relatively minor. The uninformed driver is required to perform a hard braking maneuver in order to not pass through the intersection during a red phase. The uninformed driver does not come to a complete stop as the intersection phase changes to green prior to the intersection stop line. The informed system utilizes 194 Wh/mi while the uninformed driver utilizes 393 Wh/mi to traverse the same

distance. In this case the informed system demonstrates a 51% reduction in propel energy consumption compared to the uninformed driver. Fig. 3.10 displays the informed system's response while the uninformed driver's response can be seen in Fig. A.4.

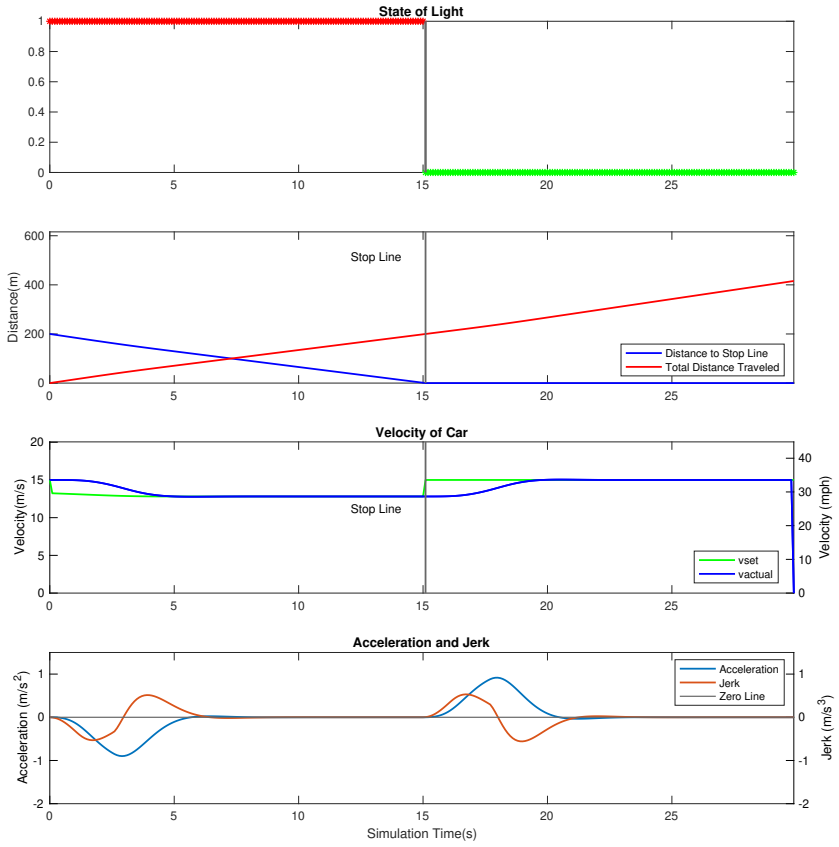

Figure 3.10: Case 5: Small Deceleration

6. **SPaT Data Received much Further Away**
   In the simulation, the informed system is able to coast down to a constant speed in order to pass through the intersection during a green phase. Once through the intersection, the informed system drives the Ego vehicle back to the original set speed. The Ego vehicle observes very little tractive effort prior to the intersection due to a large coasting event. The uniformed driver is required to perform a hard braking maneuver in order to not pass through the intersection during a red phase. The uninformed driver does not come to a complete stop as the intersection phase changes to green prior to the intersection stop line. The informed system utilizes 115 Wh/mi while the uninformed driver utilizes 230 Wh/mil. In this case the informed system demonstrates

a 50% reduction in propel energy consumption compared to the uninformed driver. The further the Ego vehicle is from the connected intersection when it starts receiving SPaT and MAP data allows for further energy reduction. This is evident when comparing Case 4 to Case 6. Fig. 3.11 displays the informed system's response while the uninformed driver's response can be seen in Fig. A.5. Fig. 3.12 demonstrates the Ego vehicle controllers following a coasting profile.

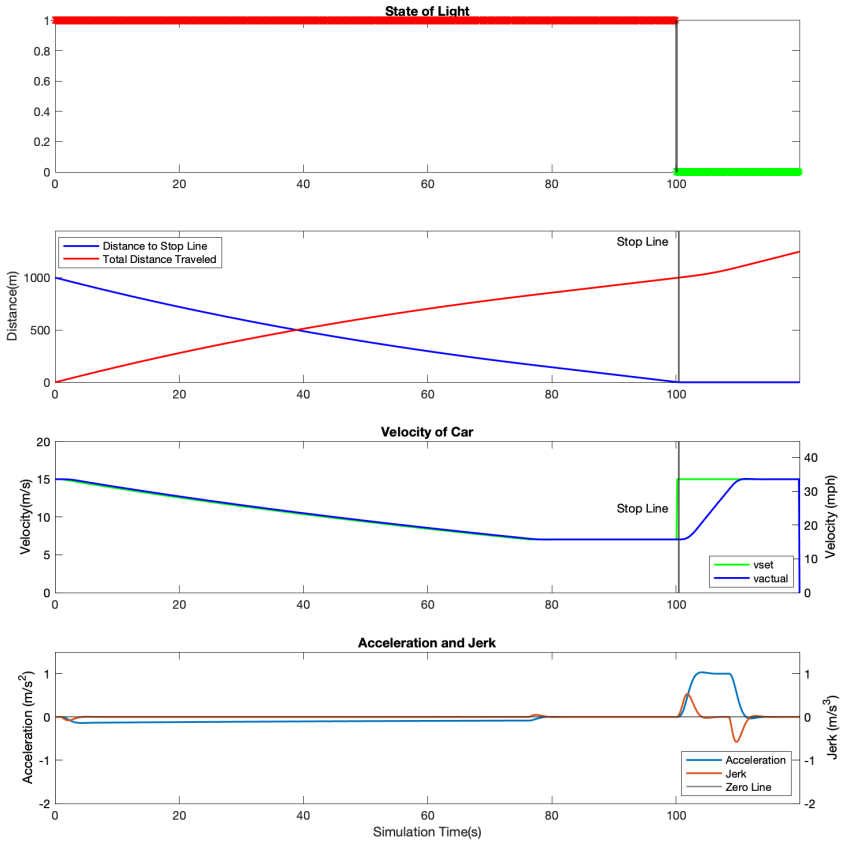

Figure 3.11: Case 6: SPaT Information Received Further Away

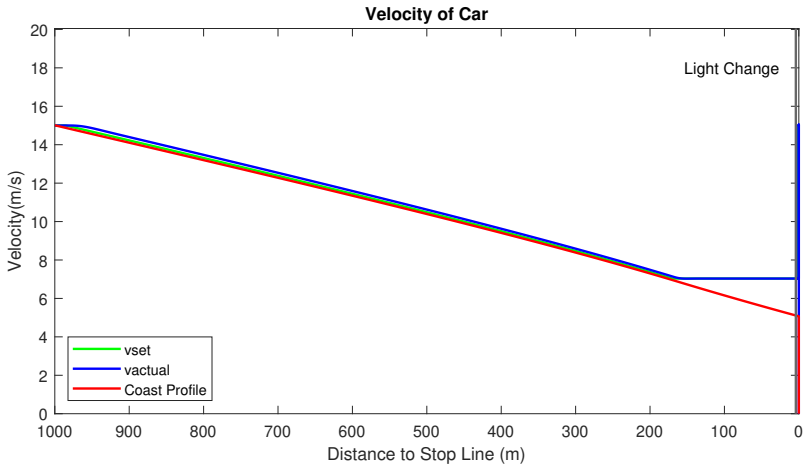

Figure 3.12: Case 6: Coasting Demonstration

Table 3.1: Summary table of energy consumption comparisons for Cases 1-6 (15 m/s).

Scenario	Propel Energy (Wh/mil)	Brake Energy (Wh/mil)	Net Energy (Wh/mil)	Travel Time (s)
Case 1	6.6	-493	-487	38
Case 1 Uninformed	81	-559	-478	31
Case 2	385	-276	109	60
Case 2 Uninformed	433	-325	107	55
Case 3	166	-16.1	150	60
Case 3 Uninformed	256	-123	133	112
Case 4	271	-147	123	40
Case 4 Uninformed	365	-244	122	42
Case 5	194	-58.4	136	30
Case 5 Uninformed	393	-274	119	34
Case 6	115	-0.1	115	120
Case 6 Uninformed	230	-93.8	136	121

Table 3.1 displays simulated energy consumption for each case in Wh/mil. The important parameters discussed in this research are propel tractive energy and travel time. However, tractive brake energy and net tractive energy at the wheel are also tracked. In a few of the cases discussed, the net tractive energy is lower in the uninformed driver scenarios. This is due to the larger braking maneuvers the uninformed driver has to perform in order to not pass through the intersection during a red phase. This however does not mean that the uninformed driver in these scenarios would consume less energy overall. Powertrain efficiencies and regen brake efficiencies could change this outcome. The outcome is also affected whether the Ego vehicle is an internal combustion engine

only or a battery electric vehicle. It is this reason that the main comparison point used in this research is tractive propel energy at the wheel.

7. **Following a Vehicle to the Intersection**
   In this simulation, the SPaT and MAP data is structured in a way so the Ego vehicle will be required to accelerate to a faster speed in order to pass through the intersection during a green phase. However, the Ego vehicle is unable to perform the speed updates from the Signalized Intersection Control Strategy due to a lead vehicle. Once this fact is realized by the system, the control strategy begins following its braking maneuver speed updates. Once close enough to the intersection, the MPC controller takes over to accurately bring the Ego vehicle to a stop at the intersection stop line. The lead vehicle is assumed to have either changed lanes or accelerated through the intersection. Fig. 3.13 displays the response of the combined Ego ACC and Signalized Intersection Control Strategy systems. While the response does show an instance of high jerk observed around the $10s$ mark in the simulation, it is only observed for an instant which is likely due to controller switching.

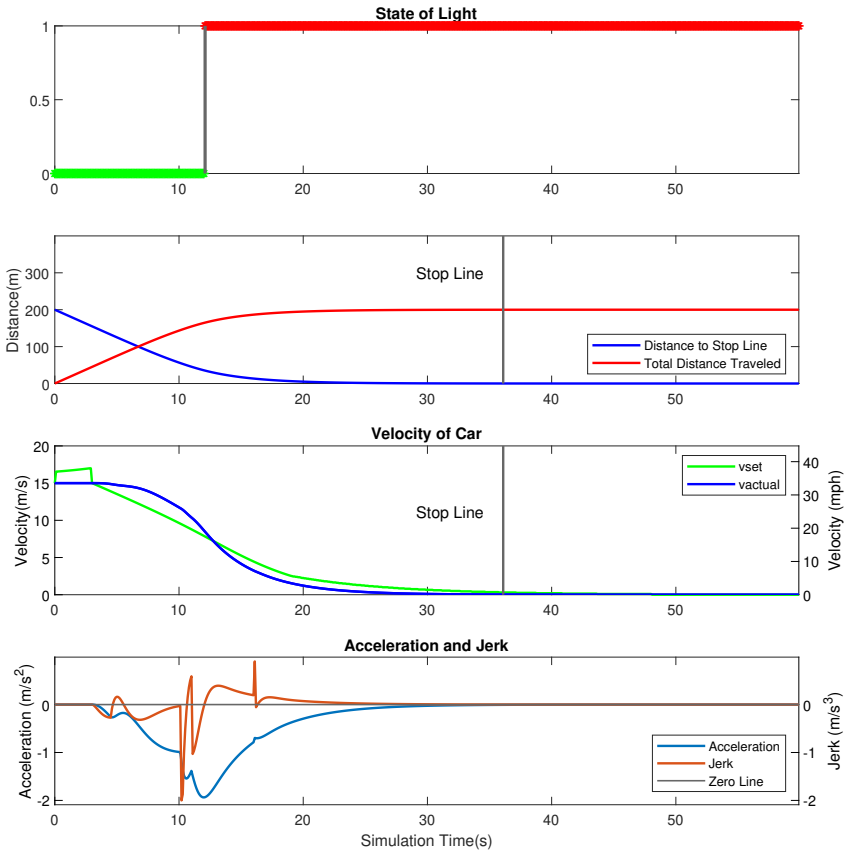

Figure 3.13: Ego Vehicle Following a Lead Vehicle to the Intersection

8. **Vehicle Cut in Prior to the Stop Line**
   In this simulation, the SPaT and MAP data is structured in a way so the Ego vehicle can maintain its original set speed in order to pass through the intersection during a green phase. However, the Ego vehicle experiences a lead vehicle cut in at close proximity traveling ($10m/s$) slower then the Ego vehicle. This stimulates an aggressive brake performed by the Ego vehicle in order to maintain safety. This results in a large observed jerk which is expected. Once the Signalized Intersection Control Strategy realizes the Ego vehicle can no longer make the intersection during a green phase, it updates set speed with its braking maneuver. Once again the MPC controller is utilized to accurately bring the Ego vehicle to a stop at the intersection stop line. The lead vehicle is assumed to have changed lanes or accelerated through the intersection. Fig. 3.14 displays the response of the combined Eco ACC and Signalized Intersection Control Strategy systems. The vehicle cut in is observable as the sharp decrease in distance to nearest object in the figure below.

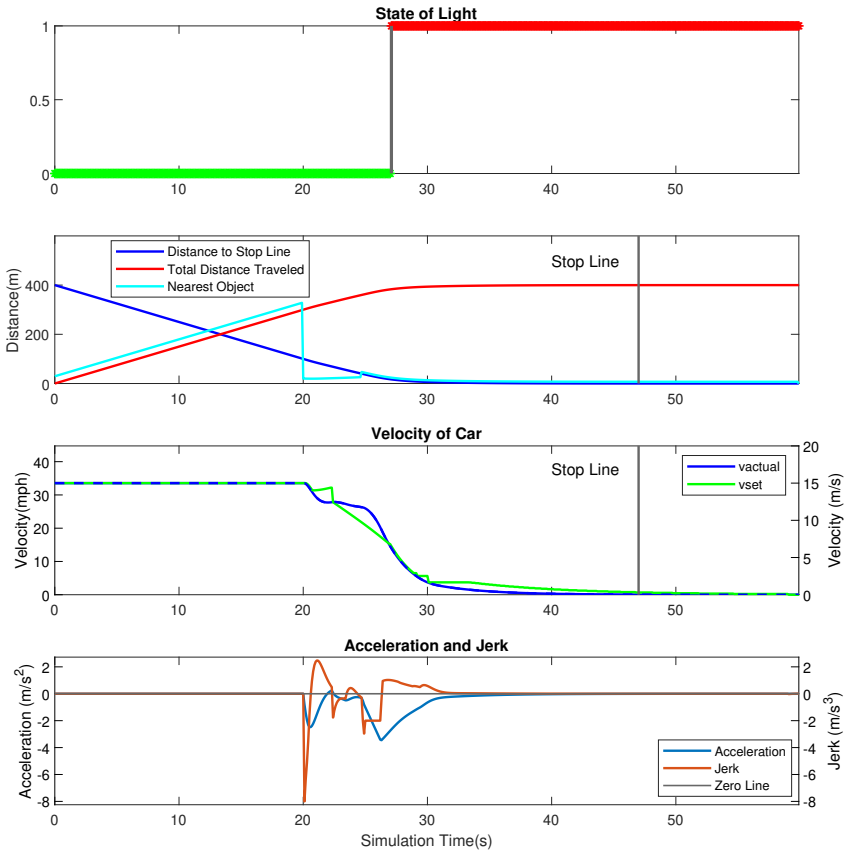

Figure 3.14: Ego Vehicle Observing a Harsh Vehicle Cut In

Chapter 4

Conclusion and Future Work

The Signalized Intersection Control Strategy shows promise in achieving reduced energy consumption at the wheel. A Signalized Intersection Control Strategy that updates the set speed of the Ego vehicle, is able to work in conjunction with an Eco ACC system to reduce energy consumption while maintaining safety and comfort of the rider. The control strategy is successfully able to update the set speed of the vehicle while working with an acceleration request cruise controller.

The Eco ACC system utilized in this research has bounded acceleration and jerk to improve rider comfort. The comfort limits are a max jerk of 0.9 m/s^3 and a max acceleration of 2 m/s^2. With a properly tuned state feedback control law, the acceleration request cruise controller converges to any set speed update forced by the Signalized Intersection Control Strategy. The standard cruise controller has been vetted through varying large disturbances such as wind gusts and changes in road grade. Next, the headway control algorithm is designed and tested. Through the simulation of both the lead and Ego vehicles, both the headway control and subsequently Model Predictive Control algorithms are tuned towards favorable results. This portion of the Eco ACC system is also jerk limited under normal circumstances to ensure rider comfort [1].

The creation of the Signalized Intersection Control Strategy begins with the knowledge of the desired inputs and outputs. There are multiple inputs into the control strategy: current Ego vehicle speed, current Ego vehicle set speed, distance to intersection stop line, current phase of the stop light, and time remaining until next phase change. The singular output of the control strategy is the next updated set speed to be utilized by the Eco ACC system. The base control strategy is segmented into different sections in order to allow changes to the control strategy to affect solely what is intended. There are three main checks being performed each time the Signalized Intersection Control Strategy function is called by the Eco ACC system. These include checking whether a full stop has been requested, if the light has changed from its initial phase, and if the current phase is green. The control strategy utilizes the results of these checks to make its decisions down stream. One of the more

important sections of the control strategy is how the vehicle is brought down to a full stop. A braking look up table is created to allow the control strategy to determine what method of closing the distance to the stop line the Ego vehicle should use. There are three options depending on the current vehicle speed and the distance to the intersection stop line. The Ego vehicle can either maintain its speed, coast, or perform active braking.

Once the base Signalized Intersection Control Strategy is developed, it needed to be tested and vetted without the added complexity of any additional vehicle controllers. Through simulation, the base level control strategy is confirmed to be updating the set speed of the system. Several tests are created to ensure every segmented section of the strategy is operating as intended. With the control strategy verified, it could now be integrated into the Eco ACC system.

With the Signalized Intersection Control Strategy integrated into the Eco ACC system, several test scenarios are developed in order to test the entire system. These include having the Ego vehicle stop at the intersection stop line with the initial phase both green and red, having the Ego vehicle both speed up and slow down slightly to make the intersection during a green phase, as well as checking the Eco ACC systems of vehicle following and vehicle cut in during an intersection approach to verify the safety of the entire system. Tractive energy at the wheel for the combined Eco ACC system and Signalized Intersection Control Strategy is compared to an uninformed driver for Cases 1-6 discussed in the research. The uninformed driver is simulated such that the vehicle maintains the original set speed until the driver observes a yellow light indicator. The uninformed driver will then begin a braking maneuver to bring the vehicle to a stop at the intersection stop line and accelerate back to the original set speed once the phase turns green. The differences in tractive propel energy at the wheel for Case's 1-6 can be seen in Table. 4.1 where propel energy reduction is the difference between the uninformed driver and the combined Eco ACC system with Signalized Intersection Control Strategy.

Table 4.1: Energy Consumption Differences for Cases 1-6 ($15m/s$).

Scenario	Propel Energy Reduction (Wh/mil)	(%)
Case 1	75	92
Case 2	47	11
Case 3	90	35
Case 4	95	26
Case 5	199	51
Case 6	115	50

Table 4.1 states that for each case, the addition of the Signalized Intersection Control

Strategy reduces the required propel tractive energy necessary to travel the simulated distance. The further away SPaT and MAP data can be received by a connected Ego vehicle, the better decisions that vehicle can make about its approach to a signalized intersection. This is evident when comparing Case 4 to Case 6. Both of these scenarios are developed such that the vehicle will slow down to a constant speed and pass through the light during a green phase. However, in Case 6 the Ego vehicle starts receiving SPaT and MAP data a little over twice the distance away which allows the Ego vehicle to coast down to a constant speed rather than performing active braking. This change accounts for much of the difference between the energy savings seen in both cases, about 50% more energy saving observed at the wheel in Case 6 over Case 4.

The implementation of the Signalized Intersection Control Strategy successfully reduces energy consumption at the wheel of the Ego vehicle. The control strategy allows the set speed of the Eco ACC system to be updated in response to SPaT and MAP data. The integration of the Signalized Intersection Control Strategy maintains the acceleration and jerk limits on the Eco ACC system. A considerable decrease in energy consumption ranging from 11% to 92% for a vehicle traveling at a set speed of 15m/s is observed. The simulated results display good functionality and suggest that the next step for testing would be implementing the Signalized Intersection Control Strategy on a vehicle.

Further examination is recommended to test the Signalized Intersection Control Strategy to determine the differences in performance of initial set speeds of the Ego vehicle. Another consideration could be to test the performance differences between an internal combustion engine and a battery electric vehicle.

A major goal in Year 4 of the EcoCAR Mobility Challenge is the implementation of longitudinal Adaptive Cruise Control with an appropriate connected intersection control scheme. Based on the current longitudinal ACC system, the addition of a Signalized Intersection Control Strategy like the one proposed in this research could be easily integrated into the background operations of the vehicle controllers. Once the new control strategy is correctly integrated, vehicle testing should be performed to validate the findings of this research. The testing of the control strategy includes potential tuning of when to switch to MPC control for accurate braking to the intersection stop line. Since the Signalized Intersection Control Strategy is able to safely drive the set speed of the Eco ACC system to maintain rider comfort, reduce tractive energy consumption, and decrease travel time of the Ego vehicle in some cases, the objectives of this research have been accomplished.

References

[1] Ryan, Timothy P (2021),"Model Predictive Adaptive Cruise Control with Consideration of Comfort and Energy Savings",MS Thesis,VPI&SU,Blacksburg, Va. https://vtechworks.lib.vt.edu/handle/10919/103744.

[2] Environmental protection agency. Automotive Trends Report, Jan 2021. https://www.epa.gov/automotive-trends/highlights-automotive-trends-report.

[3] Environmental protection agency. Data on Cars used for Testing Fuel Economy, Mar 2021. https://www.epa.gov/compliance-and-fuel-economy-data/data-cars-used-testing-fuel-economy.

[4] V. L. Bageshwar, W. L. Garrard, and R. Rajamani. Model predictive control of transitional maneuvers for adaptive cruise control vehicles. *IEEE Transactions on Vehicular Technology*, 53(5):1573–1585, 2004.

[5] Alan Brown, Marc Nalbach, Sebastian Kahnt, and André Korner. Emissions reduction via 48v active engine-off coasting. *SAE International Journal of Alternative Powertrains*, 5(1):68–78, apr 2016.

[6] Sai Krishna Chada, Ankith Purbai, Daniel Görges, Achim Ebert, and Roman Teutsch. Ecological adaptive cruise control for urban environments using spat information. In *2020 IEEE Vehicle Power and Propulsion Conference (VPPC)*, pages 1–6. IEEE, 2020.

[7] Luigi Del Re, Frank Allgöwer, Luigi Glielmo, Carlos Guardiola, and Ilya Kolmanovsky. *Automotive model predictive control: models, methods and applications*, volume 402. Springer, 2010.

[8] Mehrdad Ehsani, Yimin Gao, Sebastien Gay, and Ali Emadi. *Modern Electric, Hybrid Electric, and Fuel Cell Vehicles: Fundamentals, Theory, and Design*. 2004.

[9] Cahyantari Ekaputri and Arief Syaichu-Rohman. Model predictive control (mpc) design and implementation using algorithm-3 on board spartan 6 fpga sp605 evaluation kit. In *2013 3rd International Conference on Instrumentation Control and Automation (ICA)*, pages 115–120. IEEE, 2013.

[10] National Motorists Association Foundation. STOP Short Yellow Lights. Available:. *http://www.shortyellowlights.com/standards/*, 2022.

[11] Lino Guzzella and Antonio Sciarretta. *Vehicle Propulsion Systems, 3 Ed*, pages 67–162. 2013.

[12] Konstantinos Katsaros, Ralf Kernchen, Mehrdad Dianati, and David Rieck. Performance study of a green light optimized speed ..., 2011.

[13] E. Kural and B. Aksun Güvenç. Model predictive adaptive cruise control. In *2010 IEEE International Conference on Systems, Man and Cybernetics*, pages 1455–1461, 2010.

[14] Li-hua Luo, Hong Liu, Ping Li, and Hui Wang. Model predictive control for adaptive cruise control with multi-objectives: comfort, fuel-economy, safety and car-following. *Journal of Zhejiang University SCIENCE A*, 11(3):191–201, 2010. https://link.springer.com/article/10.1631/jzus.A0900374.

[15] MATLAB. Mpc function. https://www.mathworks.com/help/mpc/ref/mpc.html.

[16] Marek Michalczuk, Bartłomiej Ufnalski, and Lech Marian Grzesiak. Imposing constraints in a full state feedback system using multithreaded controller. *IEEE Transactions on Industrial Electronics*, 68(12):12543–12553, 2020.

[17] Patrick Phlips, Thomas Megli, and William Ruona. Unified power-based analysis of combustion engine and battery electric vehicle energy consumption. SAE Technical Paper 2022-01-0532.

[18] A. Sciarretta, G. De Nunzio, and L. L. Ojeda. Optimal ecodriving control: Energy-efficient driving of road vehicles as an optimal control problem. *IEEE Control Systems Magazine*, 35(5):71–90, 2015.

[19] Anake Umsrithong and Corina Sandu. A semi-empirical tire model for transient maneuver of on road vehicle. SAE Technical Paper 2009-01-2919.

[20] Xi Wei and Giorgio Rizzoni. Objective metrics of fuel economy, performance and driveability - a review. SAE Technical Paper 2004-01-1338.

[21] Niklas Wikström, Alejandro Ferreira Parrilla, Stephen John Jones, and Anders Grauers. Energy-efficient cooperative adaptive cruise control with receding horizon of traffic, route topology, and traffic light information. *SAE International Journal of Connected and Automated Vehicles*, 2(12-02-02-0006), 2019.

[22] Hermann Winner. Adaptive cruise control. *Handbook of Intelligent Vehicles*, page 613–656, 2012.

[23] Wuping Xin, Hasan Moonam, Mani Venkat Ala, et al. Connected eco-driving technologies for adaptive traffic signal control. Technical report, New York State Energy Research and Development Authority, 2019.

Appendix A

Additional Plots

Additional plots found in the appendix are discussed within this research paper. Fig. A.1 displays the simulation results of the uninformed driver. The vehicle is brought to a full stop at the intersection stop line.

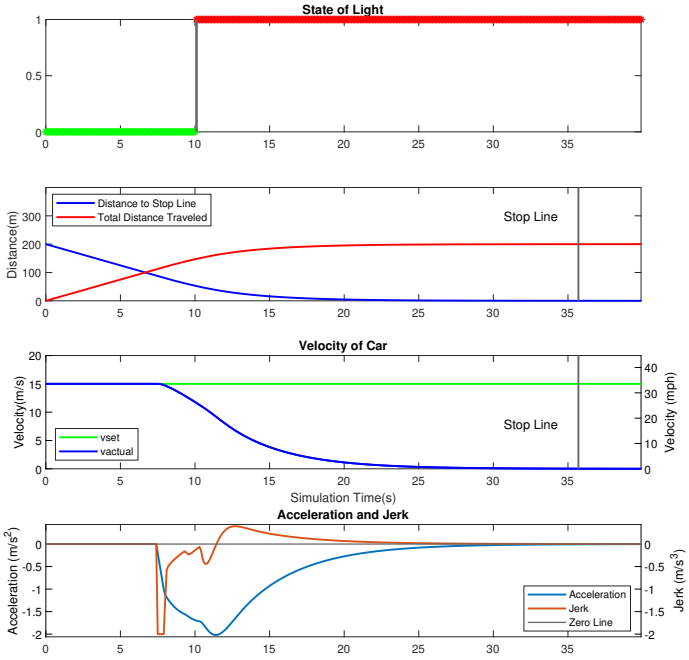

Figure A.1: Case 1 - Uninformed Driver

Fig. A.2 displays the simulation results of the uninformed driver. The uninformed driver

scenario has the vehicle participate in high acceleration and jerk maneuvers to bring the vehicle to a stop and acceleration back to the original set speed once the phase turns green.

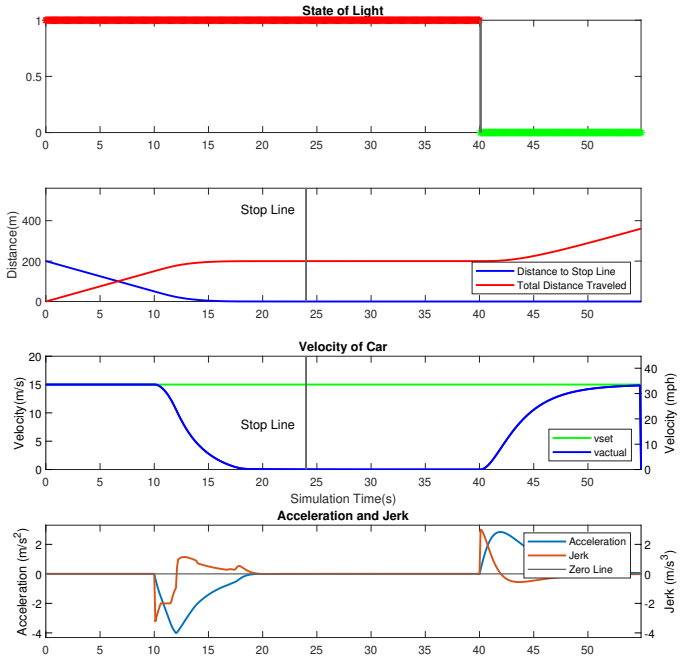

Figure A.2: Case 2 - Uninformed Driver

Fig. A.3 displays the simulating results of the uninformed driver. The vehicle shortly comes to a complete stop at the intersection stop line before the phase turns green and the vehicle accelerates back to the original set speed. This motion results in continuous high acceleration and jerk maneuvers.

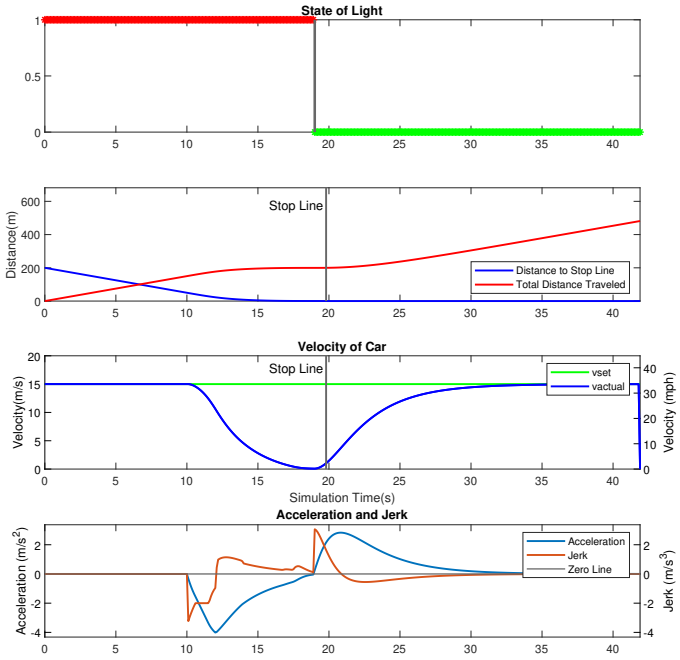

Figure A.3: Case 4 - Uninformed Driver

Fig. A.4 displays the simulating results of the uninformed driver. The vehicle brakes hard when the yellow distance matches with the current distance to the stop line. However, in this case the uninformed driver vehicle does not come to a stop. Once the phase changes to green the vehicle begins to accelerate back to the original set speed.

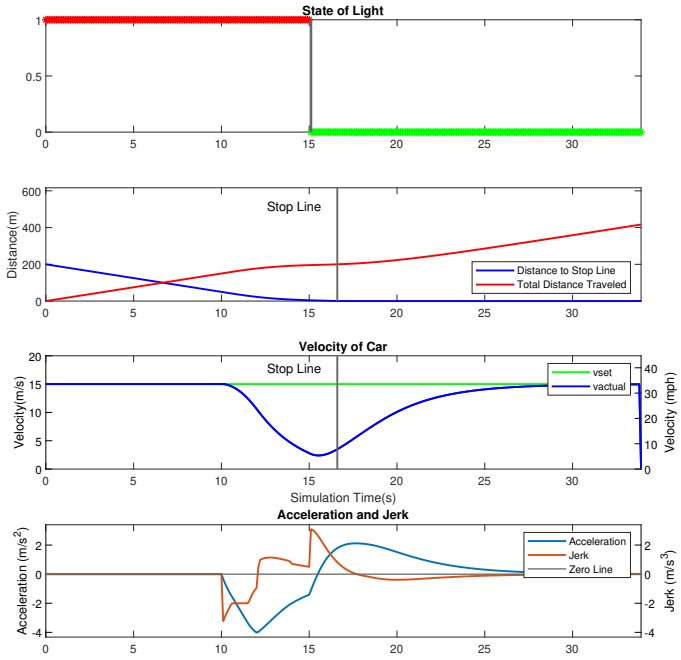

Figure A.4: Case 5 - Uninformed Driver

Fig. A.5 displays the simulating results of the uninformed driver. The vehicle travels at a constant speed until it approaches the intersection stop line while the phase of the light is currently red. The vehicle makes an abrupt full stop at the intersection and waits until the phase changes to green before accelerating back to the original set speed.

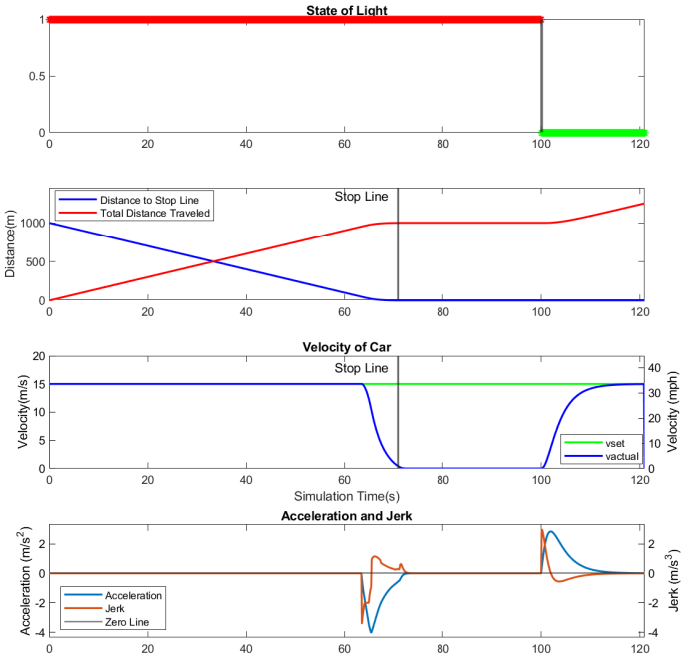

Figure A.5: Case 6 - Uninformed Driver